Ann. N.Y. Acad. Sci. ISSN 0077-8923

ANNALS OF THE NEW YORK ACADEMY OF SCIENCES
Special Issue: *Adhesion G Protein–Coupled Receptors*
ORIGINAL ARTICLE

Affinity proteomics identifies novel functional modules related to adhesion GPCRs

Barbara Knapp,[1] Jens Roedig,[1] Karsten Boldt,[2] Jacek Krzysko,[1] Nicola Horn,[2] Marius Ueffing,[2] and Uwe Wolfrum[1]

[1]Institute of Molecular Physiology, Molecular Cell Biology, Johannes Gutenberg University of Mainz, Mainz, Germany. [2]Institute for Ophthalmic Research and Medical Bioanalytics, Centre for Ophthalmology, Eberhard-Karls University Tübingen, Tübingen, Germany

Address for correspondence: Prof. Dr. Uwe Wolfrum, Institute of Molecular Physiology, Molecular Cell Biology, Johannes Gutenberg University of Mainz, J.J. Becherweg 7, 55099 Mainz, Germany. wolfrum@uni-mainz.de

Adhesion G protein–coupled receptors (ADGRs) have recently become a target of intense research. Their unique protein structure, which consists of a G protein–coupled receptor combined with long adhesive extracellular domains, suggests a dual role in cell signaling and adhesion. Despite considerable progress in the understanding of ADGR signaling over the past years, the knowledge about ADGR protein networks is still limited. For most receptors, only a few interaction partners are known thus far. We aimed to identify novel ADGR-interacting partners to shed light on cellular protein networks that rely on ADGR function. For this, we applied affinity proteomics, utilizing tandem affinity purifications combined with mass spectrometry. Analysis of the acquired proteomics data provides evidence that ADGRs not only have functional roles at synapses but also at intracellular membranes, namely at the endoplasmic reticulum, the Golgi apparatus, mitochondria, and mitochondria-associated membranes (MAMs). Specifically, we found an association of ADGRs with several scaffold proteins of the membrane-associated guanylate kinases family, elementary units of the γ-secretase complex, the outer/inner mitochondrial membrane, MAMs, and regulators of the Wnt signaling pathways. Furthermore, the nuclear localization of ADGR domains together with their physical interaction with nuclear proteins and several transcription factors suggests a role of ADGRs in gene regulation.

Keywords: G protein–coupled receptors; aGPCR; ADGR; synaptic scaffold proteins; mitochondria-associated membranes; gamma-secretase; Wnt signaling

Introduction

Over the last two decades, the adhesion G protein–coupled receptor (aGPCR or ADGR) protein family and their functional roles in cell adhesion and signaling have received increasing attention.[1] The ADGR protein family comprises 33 members, characterized by a unique protein structure composed of a large extracellular domain with adhesive function and a seven transmembrane (7TM) moiety that resembles G protein–coupled receptors (GPCRs) of the secretin family. According to the molecular signature of their 7TM domains, the 33 human AGPRs are categorized into nine distinct subfamilies (I–IX).[2]

A characteristic feature of ADGRs is their ability to undergo autocleavage at the G protein–coupled receptor proteolytic site (GPS), which is located near the first transmembrane domain and embedded in the GPCR autoproteolysis-inducing (GAIN) domain (Fig. 1A).[3] ADGR autocleavage results in an N-terminal fragment (NTF) and a C-terminal fragment (CTF) that usually stay associated as a dimer.[4] However, there is increasing evidence that the NTF and CTF can act independently.[5,6] Many CTFs show increased activation compared with the full-length receptor when overexpressed in cellular systems[7–10] and it has been presumed that the signaling function of ADGRs is regulated by their NTFs.[3,11,12] More

doi: 10.1111/nyas.14220

Ann. N.Y. Acad. Sci. 1456 (2019) 144–167 © 2019 The Authors. *Annals of the New York Academy of Sciences* published by Wiley Periodicals, Inc. on behalf of New York Academy of Sciences.

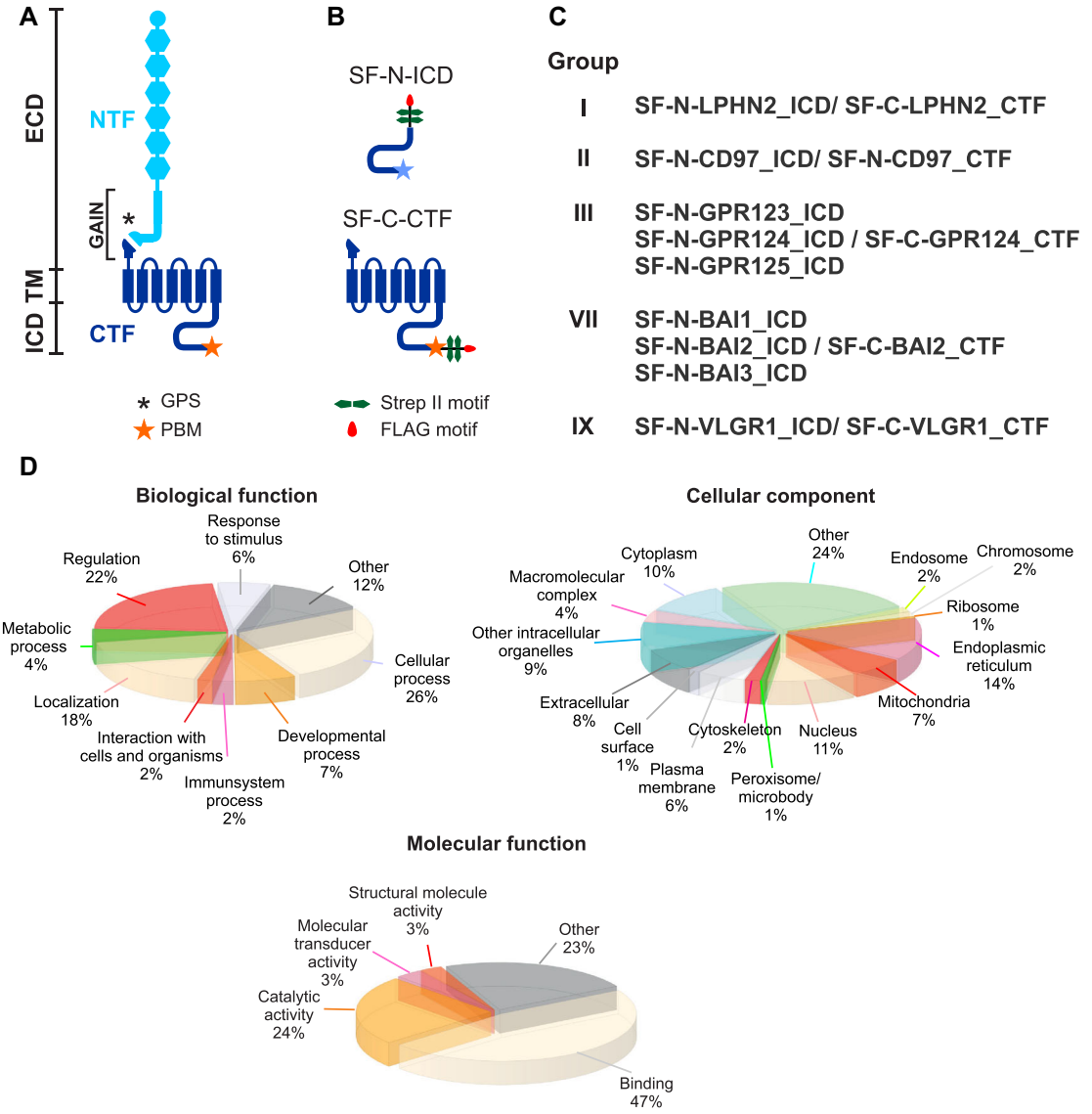

Figure 1. ADGR protein domain structure and TAP constructs and GO term analysis of TAP data. (A) General protein structure of ADGRs. (B) Schematic representation of ADGR protein fragments that were fused to a STREP II-FLAG tag. (C) ADGR fragments that were used in the TAPs. ICD, intracellular domain; TM, transmembrane domain; ECD, extracellular domain; GAIN, G protein–coupled receptor autoproteolysis-inducing domain; CTF, C-terminal fragment; NTF, N-terminal fragment; GPS, GPCR proteolytic site; PBM, PDZ-binding motif. (D) GO term analysis for ADGR TAP preys. TAP preys that are included in all ADGR_CTF datasets were grouped according to assigned GO terms using STRAP.[25] ADGR preys are mainly involved in cellular processes and regulation. They predominantly localize to the endoplasmic reticulum, nucleus, and mitochondria. The prevalent molecular functions are binding and catalytic activity.

recently, it has been demonstrated that the first ~5–10 amino acids of the CTF, called *Stachel*, mediate the activation of ADGRs upon NTF removal or conformational change.[13,14] However, there is also evidence for *Stachel*-independent signaling that requires alternative, more complex activation.[15,16]

Despite considerable progress in ADGR research, many functions of these unique receptors and their underlying molecular mechanisms remain largely elusive. The elucidation of ADGR function is hampered by the lack of known ligands and intracellular interaction partners.[17]

Identification of such interacting partners should provide a more comprehensive view of ADGR functions in defined cellular modules. In the present study, we used a powerful affinity proteomics approach to identify physically interacting partners and protein complexes of nine ADGRs from five different ADGR groups, namely LPHN2 (ADGRL2, group I), CD97 (ADGRE5, group II), GPR123 (ADGRA1, group III), GPR124 (ADGRA2, group III), GPR125 (ADGRA3, group III), BAI1 (ADGRB1, group VI), BAI2 (ADGRB2, group VI), BAI3 (ADGRB3, group VI), and VLGR1 (ADGRV1, group IX). To identify proteins and protein complexes interacting with the cellular parts of the ADGR, we tagged the intracellular domain (ICD) or CTF of the ADGRs with the Strep II/FLAG tandem affinity purification (SF-TAP) tag and expressed the SF-tagged proteins in HEK 293T cells. We subsequently performed tandem affinity purification (TAP) to isolate ADGR-associated complexes close to their native functional state from cell lysates.[18] Subsequently, the content of purified protein complexes was analyzed by liquid chromatography coupled with tandem mass spectrometry (LC–MS/MS). Analysis of the identified complex components revealed novel intracellular ADGR interaction partners, including synaptic scaffold proteins, nuclear proteins, and regulatory phosphatases. In addition, we determined for the first time the association of ADGRs with intracellular membrane networks associated with the endoplasmic reticulum (ER), the Golgi apparatus, and mitochondria. Specifically, we identified the subunits of the γ-secretase complex as a common interaction partner for VLGR1, CD97, LPHN2, and GPR124. A large overlap in the interactomes of VLGR1, CD97, and LPHN2 indicates a common joint protein interactome. Moreover, their nuclear localization paired with their physical interaction with nuclear proteins and several transcription factors suggest an unexpected role of ADGRs in gene regulation.

Materials and methods

Plasmids

Plasmids used for TAP were coding for the Strep II-FLAG (SF)-tagged versions of the following proteins: hsVLGR1 (Uniprot ID Q8WXG9-1) a.a. 6155–6306 (ICD) and a.a. 5891–6306 (CTF); hsCD97 (P48960-1) a.a. 789–835 (ICD) and a.a. 531–835 (CTF); mGPR123 (Q52KJ6-1) a.a. 202–469 (ICD); mGPR124 (Q91ZV8-1) a.a. 1066–1336 (ICD) and a.a. 745–1336 (CTF); mGPR125 a.a. 1046–1321 (ICD); mBAI1 (Q30HD1-1) a.a. 1188–1582; mBAI2 (Q8CGM1-1) a.a. 1169–1561; mBAI3 (Q80ZF8-1) a.a. 1147–1522; and mLPHN2 (Q8JZZ7-1) a.a. 1112–1487 (ICD) and a.a. 829–1487 (CTF). The cDNAs for GPR123, GPR124, GPR125, BAI1, BAI2, and BAI3 were kindly provided by Dr. Ines Liebscher (University of Leipzig); the cDNA for LPHN2 was kindly provided by Dr. Simone Prömel (University of Leipzig); and the cDNA for CD97 was kindly provided by Dr. Gabriela Aust (University of Leipzig).

Cell culture

We used HEK 293T cells, which are commonly used as human cell models for the TAP analyses,[19] including studies on GPCRs.[20] With the exception of BAI3 and GPR123, all analyzed ADGRs are expressed in HEK 293T cells[21] (VLGR1, own unpublished data). For the present experiments, HEK 293T cells and HeLa cells were cultured in Dulbecco's modified Eagle's medium containing 10% heat-inactivated fetal calf serum. Cells were transfected with GeneJuice® (Merck Millipore, Darmstadt, Germany) according to manufacturer's instructions.

Tandem affinity purification

TAP was performed as described previously,[22] allowing the isolation of protein complexes under mild conditions. For this, we tagged the N- or C-terminus of the ICDs and CTFs of ADGRs with the SF-TAP (Fig. 1A–C). SF-tagged proteins were expressed in HEK 293T cells for 48 hours. Since we observed apoptosis in the cells expressing CD97_CTF, BAI2_CTF, and LPHN2_CTF, we shortened the time of expression to 18 hours. Mock-treated HEK 293T cells were used as controls. The cells were lysed and the lysate was cleared by centrifugation. The supernatant was then subjected to a two-step purification on Strep-Tactin® Superflow® beads (IBA, Göttingen, Germany) and anti-FLAG M2 agarose beads (Sigma-Aldrich, Hamburg, Germany). Competitive elution was achieved using desbiothin (IBA) in the first step and FLAG® peptide (Sigma-Aldrich) in the second step. The eluate was precipitated by methanol-chloroform and then subjected to mass spectrometry analysis. Eluted affinity

purified complexes were subsequently analyzed by LC–MS/MS.

Mass spectrometry

LC–MS/MS was performed as previously described.[19] In brief, SF-TAP–purified protein complexes were solubilized before subjected to trypsin cleavage. The resulting peptides were desalted and purified using stage tips before separation on a Dionex™ RSLC system. Eluted peptides were directly ionized by nanospray ionization and detected by an LTQ Orbitrap™ Velos mass spectrometer (Thermo Fisher Scientific). We search the raw spectra against the human SwissProt database using Mascot and verified the results by Scaffold (version Scaffold 4.02.01, Proteome Software Inc.) to validate MS/MS–based peptide and protein identifications.

Data processing

Mass spectrometry data of all TAPs were compared with the corresponding data for mock-transfected cells. Proteins that occurred in the mock dataset were not considered for subsequent analysis. We also compared our datasets with a total of 140 TAPs of the protein RAF1, commonly used as an unrelated control TAP analysis.[18,19] Furthermore, we compared hits with the data listed in the Contaminant Repository for Affinity Purifications (CRAPome) database.[23] The CRAPome is a collection of common contaminants in affinity proteomic MS data and contains data for control experiments from an increasing number of affinity purifications. We further analyzed only those with an occurrence below 5%. The gene names of ADGR preys were used as input for the Cytoscape plugins STRING and ClueGO and the STRAP software. The parameter *confidence (score) cutout* was set to 0.4 and the parameter *maximum number of interactors* was set to 0 for STRING analysis. ClueGO v2.3.3 was used for Gene Ontology (GO) term enrichment analysis. Network specificity was set to default (medium).

Antibodies

Mouse anti-FLAG M2 (Sigma-Aldrich) and mouse anti-SIGMAR1 (sc-166392, Santa Cruz Biotechnology) were used as the primary antibodies for immunocytochemistry. Secondary antibody conjugated to Alexa568 was purchased from Molecular Probes™ (Life Technologies, Darmstadt, Germany). Nuclear DNA was stained with DAPI (1 mg/mL) (Sigma-Aldrich).

Immmunocytochemistry

Cells were fixed and permeabilized in ice-cold methanol for 10 min and washed with phosphate-buffered saline. After washing, the cells were covered with blocking solution and incubated overnight with the primary antibody at 4 °C. Cells were washed and then incubated with the secondary antibody in blocking solution containing DAPI for 1.5 h at room temperature. After washing, sections were mounted in Mowiol® (Roth). Specimens were analyzed on a Leica DM6000B microscope and images were processed with Leica imaging software and Adobe Photoshop CS (intensity adjustment). For the analysis of the colocalization of VLGR1 and SIGMAR1, the Leica DMi8 system in combination with the Thunder software was used.

Colocalization analysis

The Pearson correlation coefficient (R) was used to determinate the degree of colocalization between VLGR1_CTF_HA and SIGMAR1 in HeLa cells. Calculation of the Pearson correlation coefficient is a mathematical method to measure the strength of a linear association between two variables.[24] The correlation value has a range from + 1 to –1. A value of 0 indicates no association, greater than 0 indicates a positive association, and less than 0 indicates a negative association between the two variables. The stronger the positive association of the two variables, the closer R is to + 1. The Pearson coefficient was calculated using the Coloc 2 plugin of ImageJ (https://imagej.nih.gov/ij/).

γ-Secretase inhibitor assays

Both potent γ-secretase inhibitors LY411575 and DAPT (*N*-[*N*-(3,5-difluorophenacetyl)-L-alanyl]-*S*-phenylglycine *t*-butyl ester) were purchased from Sigma Aldrich and were added to culture media at a final concentration of 100 nM in DMSO after transfection of HEK 293T cells. As control, the same volume DMSO was added to the cells after transfection.

Results

We aimed to identify interacting partners in protein complexes associated with ADGRs by affinity proteomics in HEK 293T cells, applying TAPs in combination with mass spectrometric determination

of the protein content of eluates.[18,19] We analyzed the proteomic datasets by STRAP[25] and grouped proteins according to their assigned GO terms (Fig. 1D). We used ClueGO,[26] a Cytoscape (http://www.cytoscape.org/) plugin, for GO term enrichment analysis (e.g., Figs. S1 and S2, online only) and evaluated the specificity of the identified prey proteins by comparing our data with the CRAPome dataset. We excluded from further analyses the molecules identified in our TAPs that were in the controls and the ones that are present in the CRAPome in 5% of the datasets in order to secure a high probability of specific interaction with ADGRs.

ADGRs physically interact with scaffold proteins and synaptic proteins

Our TAP datasets reveal that ADGR subgroups I, III, VII, and IX interact with PDZ (PSD-95, discs large, zona occludens 1) domain–containing scaffold proteins (Fig. 2A). The dataset for VLGR1_ICD contained the two scaffold proteins whirlin (WHRN; previously DFNB31 or USH2D) and harmonin (USH1C). TAPs of other ADGRs revealed that the ICDs of ADGR groups III (GPR123, GPR124, and GPR125) and VII (BAI1 and BAI3) bind scaffold proteins of the membrane-associated guanylate kinases (MAGUK) family. For the BAI group, we identified CASK, LIN7C, and DLG1 (Fig. 2A). For ADGR group III, we identified the scaffold proteins CASK, DLG1, LIN7A, LIN7C, MPP2, MPP6, MPP7, and MAGI3.

In TAPs for BAI3, we also found the scaffold protein SNTB2, and for GPR124 and GPR125, we found the scaffold protein SCRIB, which was also present in TAPs of LPHN2. Both SNTB2 and SCRIB do not belong to the MAGUK family but do contain PDZ domains. In TAPs with CD97 constructs, we did not find any scaffold proteins.

Notably, we also did not identify any of the above-mentioned scaffold proteins in TAPs with the CTFs of VLGR1, BAI2, GPR124, and LPHN2, potentially due to the C-terminal SF-tag, which may block binding to the ADGR PDZ-binding motif (PBM). However, the TAP data that we acquired with ADGR_CTFs indicated synaptic localization and functions of the receptors: they contain various proteins involved in vesicle fusion and numerous interactors that are associated with synapse-related GO terms, such as *synaptic signaling* and *synaptic vesicle cycle* (Fig. 2B).

TAP data indicate binding of phosphatases and kinases to ADGRs

In TAPs of all ADGRs except GPR123, we identified diverse phosphatases and kinases (Table 1). For most ADGRs, we identified catalytic and regulatory subunits of protein phosphatases 2 (PP2) and 6 (PP6). BAI proteins also interacted with subunits of protein phosphatases 1 and 4. Interestingly, the ICDs (except in the case of VLGR1) were sufficient to interact with these phosphatases (Table 1), indicating that phosphatases preferentially bind to the ICD of ADGRs. In TAPs with CTFs of GPR124, BAI2, CD97, and VLGR1, the protein phosphatase Mg^{2+}/Mn^{2+}-dependent 1B was also found. Furthermore, our TAPs revealed casein kinase 2 (CK2), calcium/calmodulin-dependent protein kinase II (CAMK2), cyclin-dependent kinase 4 (CDK4), and mitogen-activated protein kinase 1 or 3 (MAPK1/MAPK3) as possible candidates that phosphorylate ADGRs. *In silico* analysis of ADGR amino acid sequences using the kinasephos 2.0 tool (http://kinasephos2.mbc.nctu.edu.tw/predict.php) predicts phosphorylation sites in all ADGRs studied, defining them as potential targets for phosphorylation. All ADGRs contain potential CK2 and CDK phosphorylation motifs in their ICD. A potential MAPK phosphorylation site was predicted for all ADGRs except CD97. Potential CAMK target sites were predicted for LPHN2, BAI2, and BAI3.

ADGR presence in protein complexes of the ER, the Golgi apparatus, and mitochondria

Comparing the TAP datasets of ADGR_CTFs, we identified 116 molecules present in all TAPs of all five ADGRs (Table S1, online only). We grouped these proteins according to their assigned GO terms with STRAP (Fig. 1D) and analyzed them for enriched GO terms with ClueGO (Fig. S1, Table S1, online only). Our analysis demonstrated that the most significantly enriched GO terms in the category *Cellular Component* were related to the ER, the Golgi apparatus, mitochondria, and the nucleus (Fig. S1A, online only). In the GO term category *Biological Process,* we found an enrichment in the terms *mitochondrial ATP synthesis coupled proton transport, membrane lipid biosynthetic process, protein import into nucleus*, and *response to ER stress* (Fig. S1B, online only). Notably, many of the ADGR-associated proteins were amino acid and

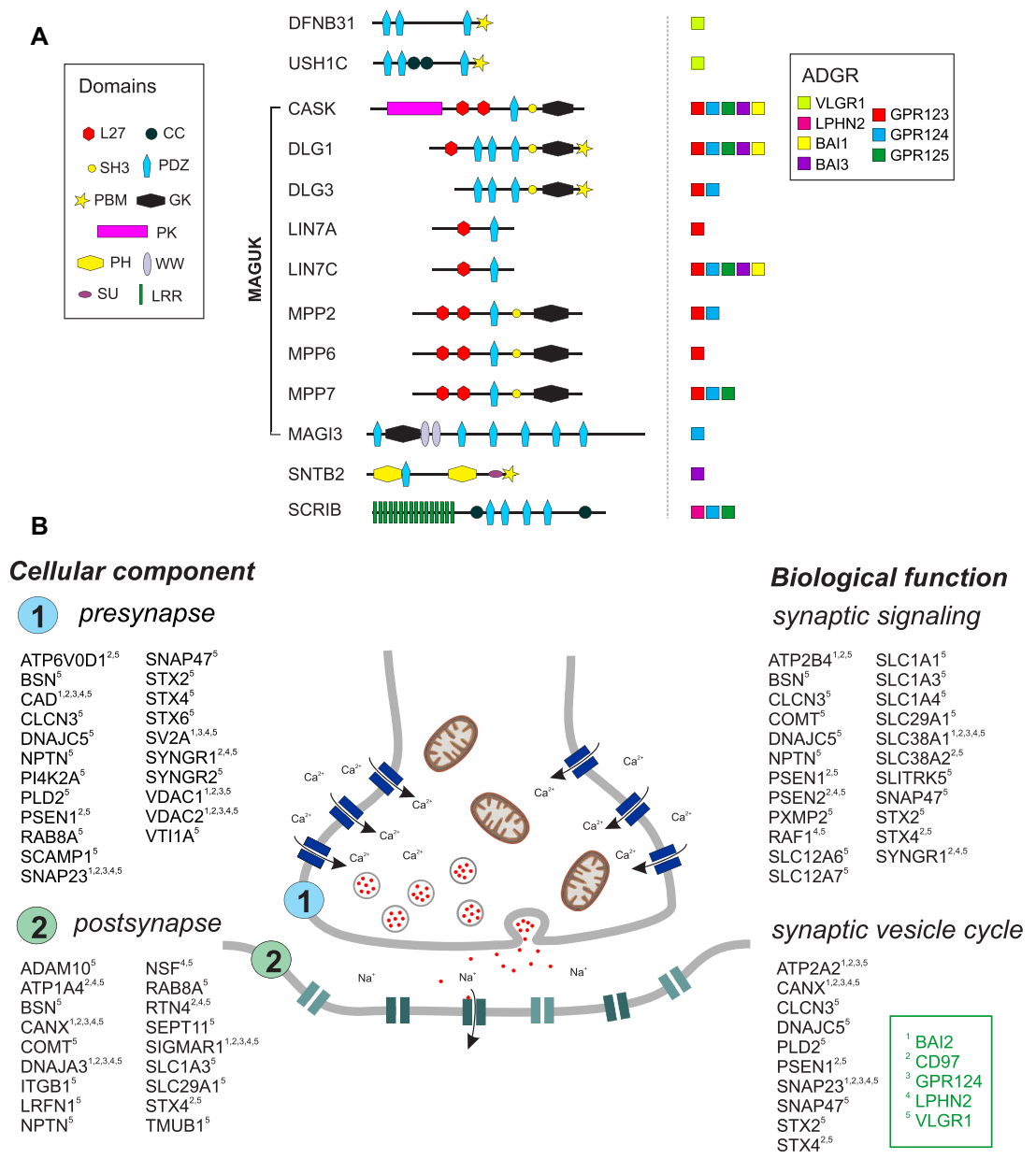

Figure 2. **ADGRs interact with scaffold proteins and other proteins associated with synaptic functions. (A) ADGR_ICDs are associated with scaffold proteins. ADGR_ICDs bind to scaffold proteins containing PDZ domains. L27, Lin2/Lin7 domain; CC, coiled-coil domain; SH3, Src homology 3 domain; PK, protein kinase; PH, pleckstrin homology; PDZ (PSD-95, DLG, ZO-1) domain; PBM, PDZ-binding motif; GK, guanylate kinase domain; WW, WW domain; SU, SU domain; LRR, leucine-rich repeat. (B) ADGR_CTFs bind to synaptic proteins. GO term enrichment analysis with ClueGO[26] reveals that TAP preys of ADGR_CTFs localize to the *pre-* and *postsynapse* and are involved in *synaptic signaling* and the *synaptic vesicle cycle*.**

zinc transporters of the solute carrier (SLC) family and ATPases that are coupled to H^+ and Ca^{2+} transmembrane transport (Table S1, online only). Several of our TAP preys were enriched in mitochondria-associated membranes (MAMs) (Table 2). MAMs are contact sites of the ER to the outer mitochondrial membrane.[27] The association with MAM proteins was most prevalent for VLGR1 and the

Table 1. Protein phosphatases and kinases identified in ADGR-TAPs

Phosphatase/ kinase	BAI1	BAI2	BAI3	CD97	GPR124	GPR125	LPHN2	VLGR1
Protein phosphatase 1		PPP1CA PPP1CC PPP1R9B						
Protein phosphatase 2	PPP2CB PPP2R1A PPP2R2A PPP2R2D	PPP2CA PPP2R2A PPP2R3A PPP2R1A* PPP2R2A*	PPP2CB PPP2R1A PPP2R2A	PPP2CA PPP2R1A PPP2R2A PPP2R1B*	PPP2CA PPP2R2A PPP2R1A*	PPP2CA PPP2CB PPP2R1A PPP2R2A PPP2R2D	PPP2CA PPP2R1A PPP2R2A PPP2R5E PPP2R1A* PPP2R1B* PPP2R2A*	PPP2R1A* PPP2R1B*
Protein phosphatase 4	PPP4C PPP4R2 PPP4R3A PPP4R3B							
Protein phosphatase 6		PPP6C PPP6R3 PPP6C* PPP6R1* PPP6R3*		PPP6C*	PPP6C PPP6R3 PPP6C* PPP6R1* PPP6R3*		PPP6C PPP6R3 PPP6C* PPP6R1* PPP6R3*	PPP6C*
Protein phosphatase, $Mg2^+/Mn2^+$ dependent, 1B		PPM1B*		PPM1G*	PPM1B*			PPM1B*
Casein kinase 2					CSNK2A1 CSNK2A2 CSNK2B CSNK2A1* CSNK2B*		CSNK2B*	
Calcium/calmodulin-dependent protein kinase II		CAMK2D CAMK2G	CAMK2D CAMK2G CAMK2D*		CAMK2D*			
Cyclin-dependent kinase 4				CDK4			CDK4	
Mitogen-activated protein kinase 1				MAPK1				MAPK1
Mitogen-activated protein kinase 3								MAPK3

Note: Listed are the phosphatase subunits and kinases that were found by TAP for each ADGR. Most subunits were identified with the ICD; those marked with * were identified with the CTF. Only those that show a low occurrence in the CRAPome (less than 5%) are listed.

least prevalent for BAI2. Immunocytochemical double labeling of VLGR1 and the MAM core protein sigma1R (SIGMAR1) in human HeLa cells transfected with VLGR1_CTF_HA revealed partial colocalization of SIGMAR1 and VLGR1 (Fig. 3C).

We also identified proteins that are located at the outer and inner mitochondrial membrane as putative interactors for all ADGR_CTFs (Table 3). These include proteins that are mainly involved in transmembrane transport and membrane folding. We found that all ADGR_CTFs associate with components of the respiratory chain, namely subunits for NADH-ubiquinone oxidoreductase (complex I), the cytochrome bc1 complex (complex III), cytochrome c oxidase (complex IV), and the F_1F_0 ATP synthase (complex V) (Fig. 3 and Table 3). In addition to components of the respiratory chain complex, we identified proteins that are involved in the assembly of mitochondrial complexes. These include COA3, OXA1L, and TIMM21, which are necessary for complex IV assembly,[28–30] as well as NDUFAF-1, -3, and -4, and TMEM126B, which participate in complex I assembly.[31–33] For VLGR1,

Table 2. Molecules related to mitochondria-associated membranes (MAMs) identified in ADGR-CTF-TAPs

Gene	Protein function	Reference	BAI2	CD97	GPR124	LPHN2	VLGR1
ACSL4	Lipid biosynthesis and fatty acid degradation	105	–	–	–	–	+
AIFM1	Apoptosis, mitochondria morphology	106	–	+	–	+	+
AMFR	Ubiquitination	107	+	+	+	+	+
BCAP31	Apoptosis	108	–	–	+	–	+
BSG	Regulatory component of γ-secretase	109	–	+	–	+	+
CANX	Calcium pumping	110	–	+	+	+	+
CISD2	Calcium homeostasis	111	–	+	–	–	+
ERLIN2	Targets IP3Rs for degradation	112	–	–	–	–	+
ERP44	ER protein retention	113	–	–	–	–	+
FUS	RNA splicing	114	+	–	+	–	–
G6PC3	Gluconeogenesis	115	–	–	–	–	+
HMOX1	Catalyzes the degradation of heme	116	–	+	–	–	–
HSPA5	ER stress, chaperone	117	–	+	+	+	+
HSPA9	Binds VDAC	76	–	+	–	+	+
LCLAT1	Cardiolipin acyl chain remodeling	118	–	–	–	–	+
LMAN1	Mannose-specific lectin	119	–	–	–	–	+
MAVS	Activation of NF-κB/IRF3	120	–	–	–	–	+
P4HB	ER protein retention	121	–	+	+	+	+
PIGN	GPI syn:transferase	118	–	–	–	–	+
PSEN1	Component of γ-secretase	122	–	+	–	–	+
PSEN2	Component of γ-secretase	122	–	+	–	+	+
PTDSS1	Phospholipid metabolism	123	+	–	+	–	+
PTDSS2	Phospholipid metabolism	123	–	+	–	–	+
RHOT1	Mitochondrial trafficking	124	–	–	–	–	+
RTN2	Generation of tubular ER	125	–	–	–	–	+
RTN4	ER–mitochondria tethering	126	–	+	–	+	+
SCD	Fatty acid transport	127	+	+	+	+	+
SIGMAR1	Lipid transport and calcium signaling	117	+	+	+	+	+
SLC27A4	Fatty acid transport	128	+	+	+	+	+
SOAT1	Cholesterol metabolism	119	–	–	–	–	+
VAPB	ER–mitochondria tethering	114	–	–	–	–	+
VDAC1	Ion exchange	76	+	+	+	–	+

Note: Only identified molecules that show a low occurrence in the CRAPome (less than 5%) are listed.

we further identified BCS1L, which is necessary for complex III assembly.[34]

All ADGR_CTFs were associated with translocases of the inner mitochondrial membrane (TIMs) and to a lesser extent with translocases of the outer mitochondrial membrane (TOMs) (Table 3). Moreover, all ADGR_CTFs bound to components of the MICOS complex that is crucial for the formation and maintenance of the mitochondrial cristae structure.[35] In addition, we found YME1L1 in TAPs for GPR124, BAI2, and LPHN2, as well as PARL for VLGR1. Both YME1L1 and PARL also maintain cristae morphology and have an antiapoptotic effect.[36,37]

CTFs of ADGR physically interact with components of the γ-secretase complex

Strikingly, we found LPHN2 as a prey for CD97_CTF and VLGR1_CTF, and CD97 as a prey for VLGR1_CTF. This indicates that these three ADGRs may be part of the same protein complexes. This prompted us to check for preys shared by CD97, LPHN2, and VLGR1 TAPs, and we found that 196 proteins were common for all three of these ADGRs (Fig. S2A, online only). After filtering out proteins that occur in more than 5% of the negative controls in the CRAPome, we performed a GO term enrichment analysis with the remaining 89 interacting proteins. Our analyses

Table 3. Molecules that localize to mitochondria identified in ADGR-CTF-TAPs

Protein	BAI2	CD97	GPR124	LPHN2	VLGR1	
Complex I NADH–ubiquinone oxidoreductase	NDUFA4 NDUFA5 NDUFA13 NDUFS1 NDUFS3	NDUFA13 NDUFA4 NDUFB10 NDUFS1 NDUFS2 NDUFS3 NDUFV1	NDUFA4 NDUFA5 NDUFS1 NDUFS2 NDUFS3	NDUFA4 NDUFA5 NDUFA9 NDUFA13 NDUFS2 NDUFS3	NDUFA4 NDUFA5 NDUFA8 NDUFA9 NDUFA11 NDUFA13 NDUFAB1 NDUFB4 NDUFB5	NDUFB10 NDUFB11 NDUFS1 NDUFS2 NDUFS3 NDUFS8 NDUFV1 NDUFV2
Complex I assembly	NDUFAF4	NDUFAF1	NDUFAF3 NDUFAF4	NDUFAF4	NDUFAF1 NDUFAF3 NDUFAF4	
Complex III Cytochrome bc1	UQCRC1 UQCRQ	UQCR10 UQCRC1 UQCRH UQCRQ	UQCRC2 UQCRQ	UQCRC2	UQCR10 UQCRB UQCRC2 UQCRFS1 UQCRQ	
Complex IV Cytochrome c oxidase	COX6C COX7B	COX4I1	COX6C COX7B	COX15 COX4I1 COX5A COX6C COX7B	COX15 COX4I1 COX5A COX6C COX7B	
Complex V F_1F_0 ATP synthase	ATP5B ATP5C1 ATP5F1 ATP5H ATP5O	ATP5A1 ATP5B ATP5C1 ATP5D ATP5F1 ATP5H ATP5O	ATP5B ATP5C1 ATP5F1 ATP5H ATP5O	ATP5C1 ATP5EP2 ATP5F1 ATP5H ATP5J2 ATP5O	ATP5A1 ATP5B ATP5C1 ATP5D ATP5EP2 ATP5F1	ATP5H ATP5I ATP5J ATP5J2 ATP5L ATP5O
MICOS complex	C19orf70	IMMT	C19orf70 IMMT	APOOL C19orf70 IMMT	APOO C19orf70 CHCHD3 IMMT	
Translocase of the inner membrane	TIMM17A TIMM21 TIMM23B TIMM50	TIMM17B TIMM23 TIMM50	TIMM17A TIMM21 TIMM23B TIMM50 TIMMDC1	TIMM17A TIMM21 TIMM23B TIMM50 TIMMDC1	TIMM17B TIMM23 TIMM50 TIMMDC1	
Translocase of the outer membrane	TOMM22	TOMM22 TOMM70A	TOMM22	–	TOMM22 TOMM40	
Mitochondrial SLC transporters	SLC16A1 SLC25A1 SLC25A10 SLC25A11 SLC25A22 SLC25A6	SLC16A1 SLC25A13 SLC25A22 SLC25A3 SLC25A5 SLC25A6	SLC16A1 SLC25A1 SLC25A10 SLC25A11 SLC25A22 SLC25A3 SLC25A5 SLC25A6	SLC16A1 SLC25A10 SLC25A11 SLC25A12 SLC25A13 SLC25A19 SLC25A22 SLC25A3 SLC25A5 SLC25A6	SLC16A1 SLC1A3 SLC25A1 SLC25A10 SLC25A11 SLC25A12 SLC25A13 SLC25A19 SLC25A21 SLC25A22	SLC25A24 SLC25A3 SLC25A33 SLC25A4 SLC25A40 SLC25A46 SLC25A5 SLC25A6 SLC27A3

Note: Only identified molecules that show a low occurrence in the CRAPome (less than 5%) are listed.

Ann. N.Y. Acad. Sci. 1456 (2019) 144–167 © 2019 The Authors. *Annals of the New York Academy of Sciences* published by Wiley Periodicals, Inc. on behalf of New York Academy of Sciences.

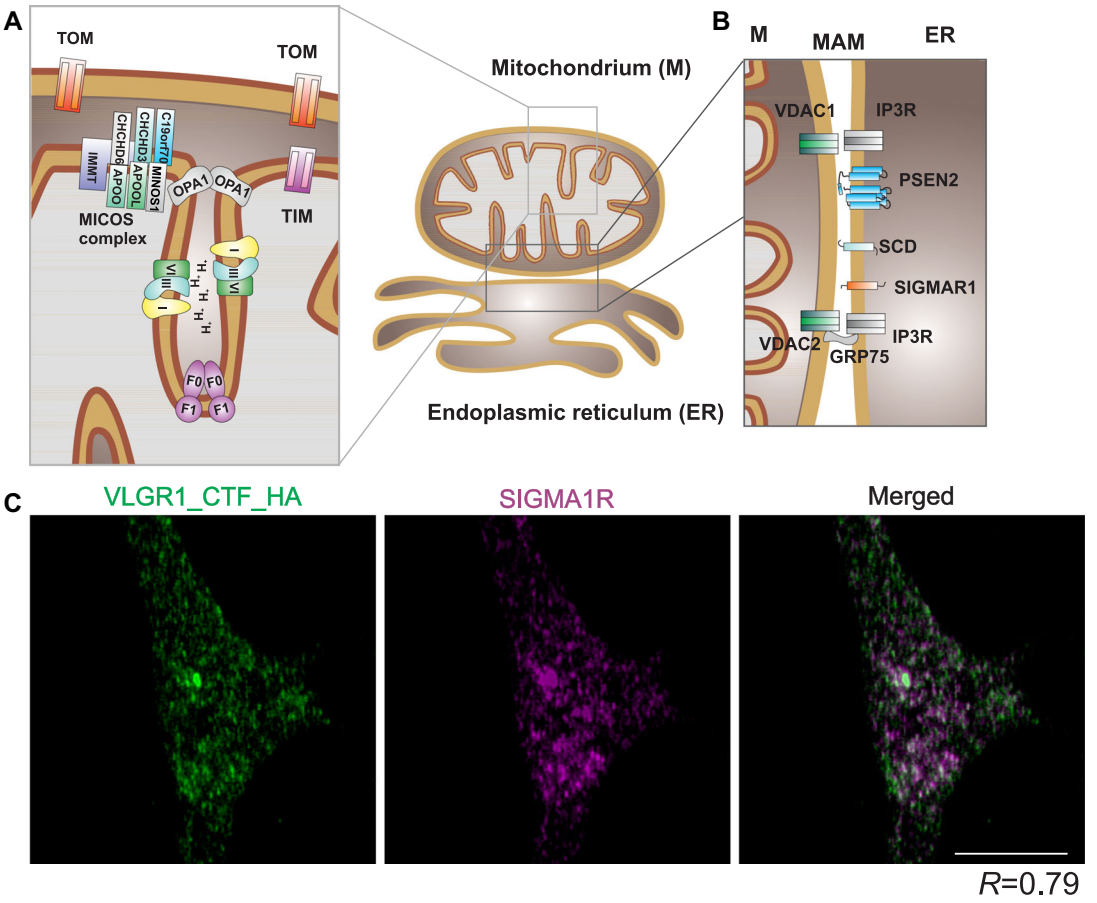

Figure 3. Mitochondrial proteins identified in ADGR TAPs. (A) Schema of mitochondria. Colored: mitochondrial proteins from the respiratory chain (complexes I, III, and IV), F_0F_1 ATP synthase, components of the MICOS complex, and translocases in the inner and outer membrane (TIMs/TOMs) (see also Table 2). Colored: proteins were identified in TAPs. Gray: other key components of mitochondrial cristae and MAMs. (B) Diverse proteins that are enriched in mitochondria-associated membranes (MAMs) were precipitated with ADGR_CTFs (see also Table 3). (C) Immunocytochemical staining of the MAM core protein SIGMAR1 and VLGR1_CTF_HA in HeLa cells reveals partial colocalization of SIGMAR1 and VLGR1. The Pearson coefficient $R = 0.79$ indicates positive association of both proteins in the cell. Exemplary analysis from three independent experiments.

revealed that the GO terms were mostly related to ER and mitochondria localization and function (Fig. S2 and Table S3, online only). We observed that all three TAPs contained subunits of the γ-secretase complex (Fig. 4A and B). Interestingly, the γ-secretase complex has recently been reported to be present in MAMs.[38–40] In TAPs of VLGR1 and CD97, we identified nicastrin (NCSTN), presenilins 1 and 2 (PSEN1 and PSEN2), as well as aph-1 homolog A (APH1A), but not presenilin enhancer 2 (PEN2), which is important for endoproteolysis of presenilins, activating the enzyme. In TAPs of LPHN2, the proteins NCSTN, PSEN2, and APH1A were present (Fig. 4B). Notably, we also found that GPR124_CTF interacts with NCSTN. In contrast, we did not identify any γ-secretase subunits in the BAI2_CTF TAP dataset.

Besides the γ-secretase complex itself, we also found several γ-secretase modulators in the ADGR TAPs. In all ADGR_CTF TAPs, the regulatory subunit basigin (BSG) was present.[41] Furthermore, we identified the presenilin cleavage proteins histocompatibility minor 13 (HM13) and the transmembrane p24 trafficking protein 10 (TMED10) in all ADGR_CTF TAPs, with the exception of BAI2 TAP.[42,43]

We further aimed to determine whether ADGRs may be substrates for the γ-secretase complex

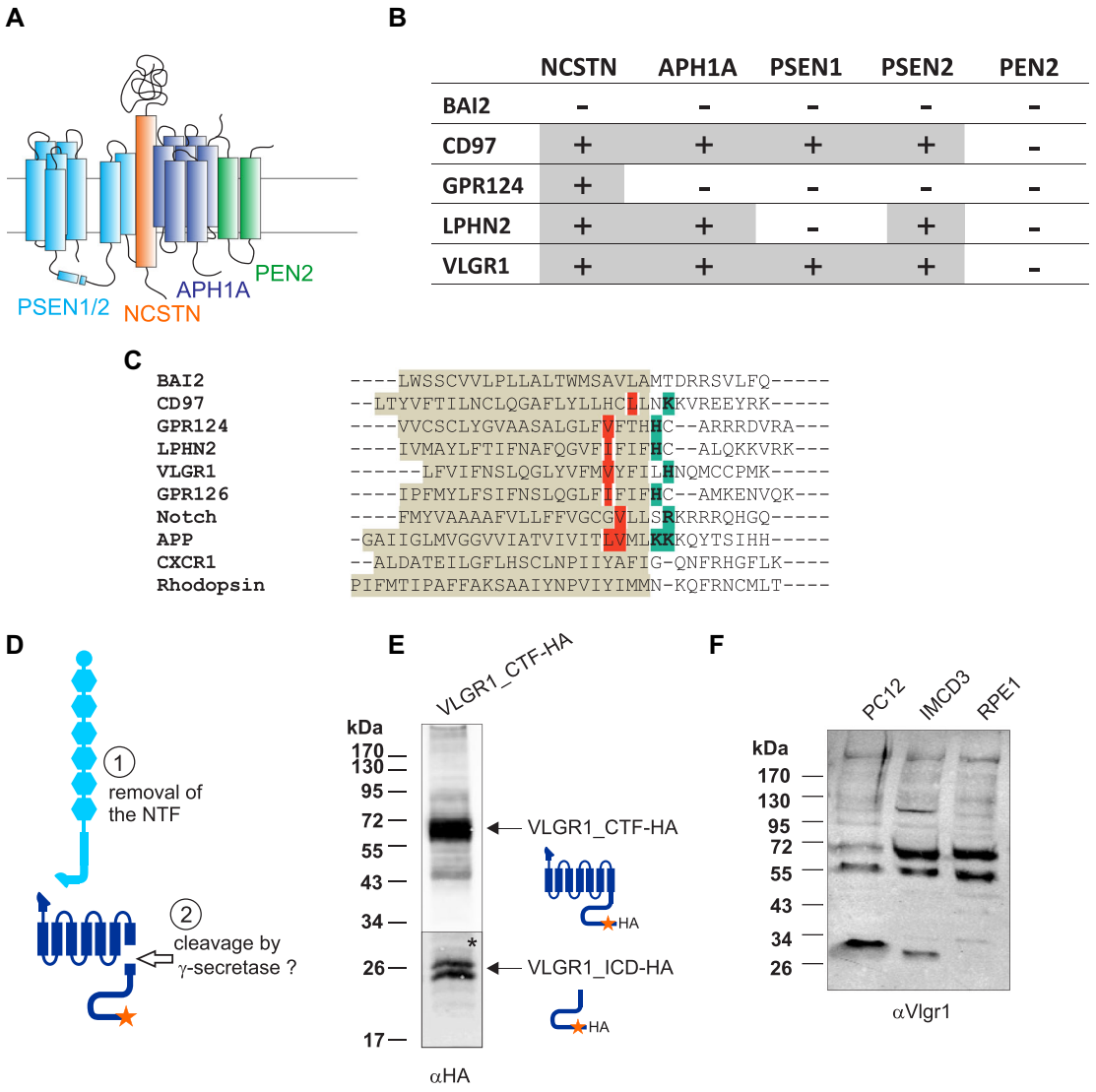

Figure 4. ADGR_CTFs bind to the γ-secretase complex. (A) Components of the γ-secretase complex: nicastrin (NCSTN), aph-1 homolog A (APH1A), presenilin 1/2 (PSEN1/2), and presenilin-enhancer 2 (PEN2). (B) Table of γ-secretase subunits that bound to ADGR_CTFs in TAP. (C) Amino acid sequence alignments of positively charged residues (colored) at the junction of the transmembrane helix 7 only of ADGRs and other receptors. Positively charged residues in Notch and APP (three to four residues after the ϵ cleavage sites) are the primary determinants for substrate binding.[44] (D) Schematic representation of ADGR cleavage by γ-secretase. (E) VLGR1_CTF-HA is cleaved, releasing a smaller band of ∼26 kDa. *The intensity of the lower part was increased relative to the upper part of the blot. (F) VLGR1-CTF and smaller VLGR1 fragments at ∼26 kDa are detected in PC12, IMCD3, and RPE1 cell lysates. Panels E and F each show an exemplary western blot from three independent experiments.

(Fig. 4C–F). Amino acid sequence alignments revealed conserved, positively charged residues at the junction of transmembrane helix 7 only in the ADGRs for which we found interactions with γ-secretase components (Fig. 4C). Charged residues located three to four residues after the ϵ cleavage sites were recently described for NOTCH and the amyloid precursor protein (APP) as the primary determinants for substrate binding.[44]

Since most γ-secretase subunits were found with VLGR1 and yet overexpression of VLGR1_CTF did not induce apoptotic effects, we chose VLGR1 for further investigation. Upon recombinant

Ann. N.Y. Acad. Sci. 1456 (2019) 144–167 © 2019 The Authors. *Annals of the New York Academy of Sciences* published by Wiley Periodicals, Inc. on behalf of New York Academy of Sciences.

expression of C-terminally tagged VLGR1_CTF-HA in HEK 293T cells, we observed that, in addition to the full-length CTF with a molecular weight of ~50 kDa, two smaller bands at ~26 kDa occurred (Fig. 4E). This size corresponds to the molecular size of the ICD of VLGR1. In addition, corresponding protein fragments were detected in cell lysates of PC12, IMCD3, and RPE1 cells (Fig. 4F).

In conclusion, these data suggested that like other γ-secretase substrates, VLGR1 is proteolytically cleaved in the transmembrane helix 7 by the γ-secretase. However, in several preliminary experiments applying well-established γ-secretase inhibitors, namely LY-411575 and DAPT, we demonstrated the inhibition of APP cleavage but did not observe any effect on ICD release from ADGRs (data not shown).

ADGRs interact with nuclear proteins and localize to the nucleus

We observed that all ADGRs studied here associated with resident nuclear proteins, which are involved in nuclear-specific functions, such as gene regulation, RNA splicing, and transcription. This was the case for both the ADGR_CTF and ADGR_ICD baits and was most prominent for GPR124, BAI1, and BAI2.

In TAPs of the GPR124_ICD and GPCR124_CTF, we found an enrichment of proteins that were assigned to the GO term *nuclear speckles*, the chromatin-free nuclear compartment of RNA splicing. For GPR124_CTF and BAI2_CTF, we observed an enrichment in proteins assigned with the GO term *nucleolus,* the site of ribosomal RNA transcription. Furthermore, the ICDs of BAI1 and GPR124 interacted with the PAF1 complex, which is involved in RNA polymerase II transcription elongation and transcription-coupled histone modifications.[45] GO terms related to histone modification, splicing, and DNA unwinding were enriched for all ADGRs; however, the numbers greatly varied.

BAI1_ICD, GPR124_CTF, GPR124_ICD, BAI2_CTF, LPHN2_ICD, CD97_ICD, and CD97_CTF were additionally associated with karyopherins (importins), which mediate nuclear import. Strikingly, we observed that the ICDs of GPR123, GPR124, GPR125, and BAI2 clearly show nuclear localization when they are recombinantly expressed in HEK 293T cells (Fig. 5A). GPR123_ICD, GPR124_ICD, and GPR125_ICD show a punctate-like enrichment in the nucleus, resembling nuclear speckles, whereas BAI2_ICD showed much larger nuclear accumulations.

The association with nuclear import proteins and the nuclear localization of some of the ADGR_ICDs led us to check whether ADGR_ICDs contain nuclear localization sequences (NLSs). For this, we applied the NLS prediction tool cNLS Mapper.[46] We found high scores for BAI1 and BAI2 and medium scores for BAI3 and GPR123. GPR124, GPR125, and LPHN2 gave only low scores, whereas no NLSs were predicted for VLGR1 and CD97 ICDs (Fig. 5B).

The results from our TAPs, together with our immunocytochemical localization analysis and the presence of NLS in some ADGRs, indicate that the ICDs of ADGRs may be cleaved and potentially act as transcription factors in the nucleus. We therefore checked our TAP data for proteins that act as transcriptional regulators. Indeed, we found numerous proteins that are related to transcriptional regulation. The molecules involved in transcriptional regulation identified in our ADGR TAPs are included in Table 4.

Identification of modulators of the Wnt signaling pathway in ADGR TAPs

The GO term analyses of our TAP data also revealed an enrichment for the GO term *Wnt signaling* in the BAI2_CTF, GPR124_CTF, and VLGR1_CTF datasets. Furthermore, single proteins involved in Wnt pathways were also found in TAPs of CD97_CTF and LPHN2_CTF (Table 5). Most of these molecules modulate Wnt signaling by targeting β-catenin. Some prey proteins have functions in the nucleus. SLC30A9 is part of the β-catenin transcription complex and participates in the regulation of Wnt downstream genes.[47]

Discussion

In the present study, we identified previously described binding partners and numerous novel putative interactors of ADGRs by TAPs in combination with subsequent mass spectrometry. Nevertheless, our affinity capture approach bears limitations, which have to be considered for the interpretation of our datasets. In our study, we used HEK 293T cells as established human cellular models for the ADGR TAPs.[19,20] Therefore, we were not able to capture tissue- or cell-specific interacting partners that are

Table 4. Molecules involved in transcriptional regulation identified in ADGR TAPs

Gene	Protein function	References	BAI2 ICD	CD97 ICD	GPR124 ICD	LPHN2 ICD	VLGR1 ICD
BTAF1	Regulates transcription in association with TATA binding protein (TBP)	129	–	–	+	–	–
BZW1	Enhances histone H4 gene transcription	130	+	+	+	+	+
BZW2	Controls translation by inhibition of eIF2	131	–	+	–	+	+
HOXA5	Transcription factor, essential for embryonic development and the nervous system	132	+	–	+	–	–
MAGEA1	Acts as an transcriptional repressor	133	–	–	+	–	–
MLF1	Posttranscriptional inhibitor and activator of gene expression	134	+	–	+	+	–
PREB	Transcription factor, probable role in cell fate	135	+	+	+	+	+
TCF25	Transcription factor important for embryonic development	136	+	–	+	+	–
UBR2	E3 ubiquitin-protein ligase plays a critical role in chromatin inactivation	137	+	–	–	+	–
UBR5	Involved in maturation and/or transcriptional regulation of mRNA	138	+	–	–	–	+

Gene	Protein function	References	BAI2 ICD	CD97 ICD	GPR123 ICD	GPR124 ICD	LPHN2 ICD	VLGR1 ICD
CTR9	Component of the PAF1 complex required for Hox gene transcription	139	+	–	–	+	–	–
ELOB	Activates elongation by RNA polymerase II	140	–	+	–	–	+	–
FHL2	Inhibits the transcriptional activity of FOXO1	141	–	–	–	–	+	+
HMGN5	Nucleosomal binding and transcriptional activation	142	+	–	–	–	–	–
MAPK1	Transcriptional repressor	143	–	–	–	–	+	+
MAPK3	Regulation of transcription factors	144	–	–	–	–	–	+
SETD7	Transcriptional activation of genes (e.g., collagenase and insulin)	145	–	–	–	+	–	–
SIRT1	Regulates epigenetic gene silencing	146	+	–	–	+	+	–
TCEAL1	Modulates various viral and cellular promoters	147	–	–	+	–	+	–

Note: Only identified molecules that show a low occurrence in the CRAPome (less than 5%) are listed.

Ann. N.Y. Acad. Sci. 1456 (2019) 144–167 © 2019 The Authors. *Annals of the New York Academy of Sciences* published by Wiley Periodicals, Inc. on behalf of New York Academy of Sciences.

A

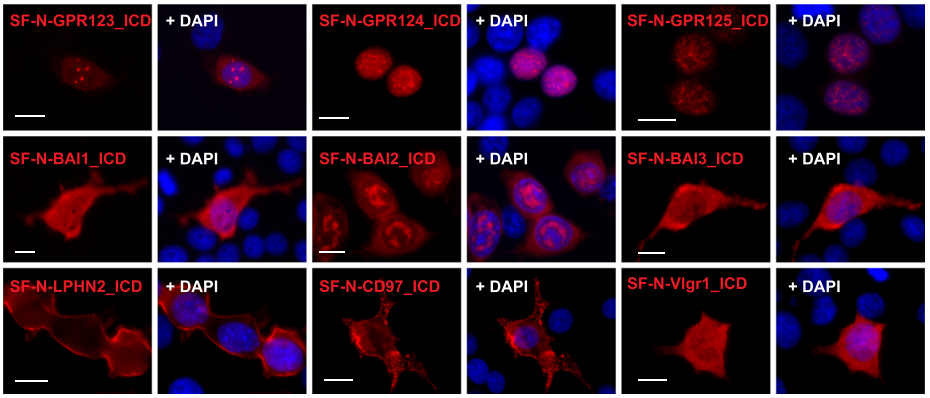

B

ADGR_ICD	NLS type	Sequence	Score*	aa
mGPR123	Bipartite	AKREDVWQCWWSCCPSRGDTSTTKPGAHP	4.5	313-341
mGPR124	Monopartite	ERESKRRSYPL	3.0	1285-1305
	Bipartite	RRRDVRASWRACCPPASPSASHVPARALP	3.0	1069-1097
mGPR125	Bipartite	GPVKSNGQEGPLLATDVTGNVRTGLWKHETT	2.2	1279-1309
mBAI1	Bipartite	RKRHQDMFQDLNRKLQHA	8.5	1487-1504
mBAI2	Monopartite	GSLERKKLRYSDLDF	7.0	1451-1465
mBAI3	Bipartite	RKRHMELFQELNQKFQTLD	6.5	1431-1449
mLPHN2	Monopartite	LYQPQKKVKPE	3.5	1364-1384
hsCD97	-	-	-	-
hsVLGR1	-	-	-	-

Figure 5. **Localization of ADGR_ICDs in the nucleus. (A) Immunocytochemical staining of SF-tagged ADGR_ICDs expressed in HEK 293T cells by anti-FLAG antibodies. Exemplary analysis from three independent experiments. (B) Predictions of nuclear localization signals (NLS) in ADGR_ICDs. *Scores: 8–10, exclusively localized to the nucleus; 6–7, partially localized to the nucleus; 3–5, localized to both the nucleus and cytoplasm; 1–2, localized to the cytoplasm. Scale bars, 10 μm.**

not expressed in HEK 293T cells. Since we cultured the cells under standard conditions, we also missed proteins that require specific physiological conditions for binding to ADGRs, such as mechanical or chemical ligand stimulation. Although TAP protein complexes are purified in close-to-native conditions, the membrane protein complexes lose their membrane context during the purification steps and therefore are difficult to obtain in general.[20] In addition, overexpression of ADGR domains may lead to changes in the stoichiometry of purified protein complex compositions. In any case, as in other screens, it is necessary to validate all newly identified putative binary interactions by applying independent, complementary experiments from the molecular to organismic level to sort out false positive hits. Nevertheless, the obtained datasets highlight the usefulness of our affinity capture approach even for membrane proteins. The identified ADGR-interacting proteins support previously discussed functions of ADGRs, but more importantly define novel physiological functions related to ADGRs.

ADGR subfamilies interact with scaffold proteins

The TAP data of our study reveal numerous interactions of ADGRs and scaffold proteins. All identified scaffold proteins possess PDZ domains and all ADGRs investigated in the present study contain a PBM at their C-terminal end (Fig. 1) that is predetermined to bind to PDZ domains. Therefore, their mutual interaction most probably occurs via the binding of ADGRs' PBM to PDZ domains. This is also confirmed by previous experimental data. We have previously shown that VLGR1 (USH2D) directly binds the two other Usher syndrome proteins, harmonin (USH1C) and whirlin (USH2D), both of which serve as cytoplasmic anchors in

Table 5. Modulators of the Wnt signaling pathway identified in ADGR TAPs

Gene	Protein function	Reference	BAI2 CTF	CD97 CTF	GPR124 CTF	LPHN2 CTF	VLGR1 CTF
AMER1	Regulator of the canonical Wnt signaling pathway	148	+	–	+	–	–
ATP6AP2	Functions as an adaptor between Wnt receptors and V-ATPase	149	–	–	–	–	+
LRP1	Represses canonical Wnt signaling	150	–	–	–	–	+
PSEN1	Inhibitor for β-catenin	151	–	+	–	–	+
PTK7	Modulates Wnt signaling activity via LRP6	152	–	–	–	–	+
RRM2	Inhibits Wnt signaling	153	–	–	–	–	+
SKP1	Mediates degradation of β-catenin	154	–	–	–	–	+
SLC30A9	Participates in transcriptional activation of Wnt-responsive genes	47	–	–	+	–	+
UBR5	Ubiquitinates and upregulates β-catenin	155	+	–	+	–	+
USP34	Regulates axin stability	156	–	–	+	–	–
WLS	Regulates Wnt protein sorting and secretion	157	+	+	+	+	+

Note: Only identified molecules that show a low occurrence in the CRAPome (less than 5%) are listed.

membrane adhesion complexes of the inner ear hair cells and retinal photoreceptor cells.[48–50] It has also been reported previously that BAI1 and GPR124 interact with DLG1 (SAP97).[10,51] Interestingly, although the direct interaction of DLG1 with the C-terminal PBM of CD97 has been shown recently,[52] we did not find DLG1 or any other PDZ-containing protein in our TAPs of CD97. This is most probably due to the fact that the interaction of DLG1 with CD97 is induced by phosphorylation of the PBM of CD97. However, this phosphorylation is induced by mechanical stimulation, a condition not present in our TAPs. Nevertheless, our TAP data revealed the interaction of ADGRs of group I (latrophilins), group III (GPR123, GPR124, and GPR125), and group VII (BAIs) with the same set of scaffold proteins (Fig. 2B). The question of whether the ADGRs are integrated in common protein networks and signaling hubs organized by scaffold proteins in cells and tissues will be reserved for future studies.

ADGR subfamilies are part of protein networks at synapses

Although the identified scaffold proteins are ubiquitously expressed, they are essential components of the protein networks of synapses, particularly of the postsynaptic density of neurons.[53] These scaffold proteins are mainly members of the MAGUK family, which are involved in the establishment and maintenance of cell polarity and the dynamic arrangement of receptors and channels at synaptic membranes.[10,54,55] In addition, we identified several proteins involved in the targeting and fusion of synaptic vesicles as putative interaction partners of ADGRs (Fig. 2B), suggesting an involvement of ADGRs in these processes too. For example, SNAP23, which interacts with all ADGR_CTFs, is known to be involved in the exocytosis of glutamate receptors to the postsynaptic membrane.[56] Our findings are also in line with the enrichment of ADGRs, namely VLGR1, latrophilins, and BAIs, at the postsynapse of dendrites[50,57–59] and the function of latrophilins and BAIs in synaptic remodeling.[55,60–62] Although the ADGRs CD97, GPR123, GPR124, and GPR125 have not been mapped to synaptic subdomains, a role in synaptic function cannot be ruled out yet.

ADGR interaction with the γ-secretase complex

Our TAP data for the ADGR_CTFs also revealed a close relationship of ADGR with the γ-secretase complex. With the exception of BAI2, we identified subunits of the γ-secretase complex in the TAPs of all other ADGR_CTFs, indicating their close

relationship with this intramembranous complex. The γ-secretase complex is well known for the generation of the β-amyloid peptide protein by the sequential proteolysis of the APP, which is a crucial step in the development of Alzheimer's disease.[63] However, in addition to APP, the γ-secretase also proteolytically cleaves a variety of integral membrane proteins that initiate downstream pathways involved in transciptional regulation in the nucleus.[64] Indeed, we also observed the release from several ADGRs of a fragment with the size of the ICD in cultures of diverse cell lines (Fig. 4). In addition, we demonstrated the localization of ADGR fragments in the nucleus, which is further supported by the presence of NLS sequences in the ICDs of diverse ADGRs (Fig. 5). Together, our findings suggest a novel signaling mechanism of ADGRs that comprises the release of an ICD upon γ-secretase cleavage and subsequent translocation of the ICD into the nucleus for gene regulation. This scenario is similar to the described signaling pathway related to the γ-secretase substrate polycystin 1 (PKD1).[65] PKD1 shows high structural similarity to ADGRs: it is also a multispanning transmembrane protein that undergoes autocleavage at a GPS, analogous to ADGRs.[66,67] Upon γ-secretase cleavage, a small (∼30 kDa) PKD1_ICD fragment is released and directed into the nucleus.[68,69] The release of PKD1_ ICD is most probably induced by mechanical stimuli,[68] an activation mechanism that has also been discussed for ADGRs.[70–72]

Although our data favor a noncanonical signaling pathway triggered by γ-secretase cleavage, our approach of applying established γ-secretase inhibitors did not alter the release of ICDs from the ADGR. ADGRs may alternatively play a role in γ-secretase positioning in specific membrane domains (e.g., lipid rafts) or in its regulation. This is supported by the fact that, besides γ-secretase subunits, we also identified γ-secretase regulators in our TAPs, such as BSG, TMED10, and HM13. In particular, BSG was found in the TAP datasets for LPHN2, CD97, and VLGR1 CTFs and was previously described as a potential additional γ-secretase regulatory subunit.[41] TMED10 was present in all ADGR_CTF TAPs except for BAI2. It is part of presenilin complexes and regulates γ-secretase cleavage activity.[73] Finally, HM13 was identified as a TAP prey for all ADGR_CTFs. It is an activator for PSEN1 and thereby promotes γ-secretase cleavage.[43]

In any case, our TAP data revealing the interaction of ADGR with the γ-secretase complex pave the way for further investigations to identify the role of this interplay. Interestingly, the γ-secretase complex is not only present in the plasma membrane but is even more prominently associated with internal cell membranes, such as the ER or MAMs.[38–40]

Evidence for association of ADGRs with MAMs and participation at biogenesis of mitochondria

In the present TAPs, we identified many proteins known to locate mainly to specific intracellular compartments, such as the ER and mitochondria. The high number of molecules related to intracellular compartments suggests novel roles of ADGRs in the cell that have not been described so far. In particular, we found various proteins located at contact sites between the ER and mitochondria, namely the MAMs. Interestingly, the γ-secretase subunits PSEN2 and PSEN1 are enriched in this compartment. Besides γ-secretase subunits, we identified the MAM protein SIGMAR1 as an interactor for all ADGRs analyzed. The present immunocytochemistry demonstrates partial colocalization of this MAM core protein with VLGR1. SIGMAR1 regulates ITP3R-dependent calcium efflux at the ER and the biogenesis of lipids.[74] The spatial regulation of calcium homeostasis and lipid biogenesis are both major processes associated with MAMs.[27,75] In addition, our analyses of TAPs indicate that all ADGRs interact with the voltage-dependent anion channels 1 and 2 (VDAC1 or VDAC2) that localize to the outer mitochondrial membrane and allow the exchange of small hydrophilic molecules.[76,77] It is conceivable that ADGRs assist in the function of the highly dynamic MAMs.[78]

Surpisingly, we identified various ADGR interactors that localize to the mitochondrial inner membrane. The majority of the identified mitochondrial proteins have very low occurrence in the CRAPome, indicating the specificity of their interaction with ADGRs. These TAP hits are subunits of the respiratory chain complexes I, III, and IV, as well as subunits of the F_0F_1 ATP synthase, all localizing to mitochondrial cristae (Fig. 4).[79,80] In

addition, we identified components of the MICOS complex, which is essential for cristae formation,[35] and proteins that are involved in complex assembly of the respiratory chain. Furthermore, we found inner and outer membrane translocases (TIMs and TOMs), which are essential for transmembrane translocations.

ADGRs have not been found in mitoproteomes so far.[81,82] However, a previous report indicated a substantial role of GPR126, a group VII ADGR, in the biogenesis of mitochondria.[6] GPR126 deficiency results in mitochondrial defects in the developing heart of mice. These defects manifest in defective differentiation of mitochondrial cristae. The present identification of putative ADGR interactors that are localized to cristae or support the formation of cristae suggests that ADGRs may regulate the biogenesis of mitochondria in general. Patra *et al.*[6] also observed the accumulation of lipids in *Gpr126*$^{-/-}$ cardiomyocytes, indicating defective lipid metabolism. This is in line with a function of ADGRs in MAMs, which are very important for lipid biogenesis and represent sites of constant lipid exchange.

It is noteworthy that the respiratory chain subunits that we identified are all transcribed in the nucleus and have to be imported into mitochondria. There is growing evidence that MAMs play an essential role in this translocation processes. Based on our findings, we hypothesize that ADGRs are part of the dynamic MAMs and participate in the control of the delivery of mitochondrial components into mitochondria during mitochondrial biogenesis. For this, they may interact only transiently with mitochondrial proteins, which may also explain why ADGRs are not present in the existing mitoproteomes.

TAP data indicate regulation of ADGRs by phosphorylation

The identification of diverse kinases and phosphatases in the present TAPs (Table 1) indicates that both kinases and phosphatases bind to ADGRs. ADGRs may serve as scaffolds for these enzymes. Alternatively, they may regulate the ADGR function by the yin and yang of protein phosphorylation and dephosphorylation. The latter hypothesis is supported by previous data demonstrating that extracellular domain phosphorylation may facilitate ADGR signaling.[12] However, most putative phosphorylation sites have been identified in the ICD of ADGRs.[12] This is also in line with the predicted phosphorylation sites of all kinases identified by the present TAPs. The phosphorylation of residues in the PBMs of the ICD may regulate the binding to PDZ domains of diverse scaffold proteins also identified as potential interactors in the present study (see above). Such regulation has recently been described for the binding of CD97 to one of the PDZ domains of the DLG1 scaffold protein triggered by the phosphorylation of the C-terminal PBM of CD97.[52] This mechanism might be a general mechanism for the regulation of PBM and PDZ domain interaction.

It is notable that we did not identify any member of the GPCR kinase (GRK) family by TAPs. GRKs phosphorylate activated canonical GPCRs, which promotes the binding of arrestins, precluding further G protein coupling.[83] GRKs phosphorylate GPCRs usually at serine, threonine, or tyrosine residues present in the third intracellular loop of the 7TM domain and the ICD. However, GRKs for ADGR phosphorylation have not been identified so far. Therefore, the absence of GRKs in our TAPs can be due to the fact that we did not stimulate the ADGRs in our TAPs or that indeed no GRKs exist for ADGRs.

The identified kinases are part of signaling pathways, which may be related to ADGR. For example, MAPK1 and MAPK3 (also known as extracellular signal–regulated kinases (ERK1/2)) are central kinases of the ERK pathway that plays an important role in integrating external signals into signaling events promoting cell growth and proliferation in many mammalian cell types.[84] One of the targets of the MAPK/ERK kinase cascade is another identified kinase, CDK4, which controls the G_1-S phase in the cell cycle. The elucidation of the role of ADGRs and their putative interacting kinases in signaling pathways has to be reserved for future experimental investigations.

ADGRs interact with Wnt/planar cell polarity signaling proteins

Our TAP data provide several lines of evidence that ADGRs are modulators of Wnt signaling. This is in line with previous reports describing crosstalk between the Wnt and ADGR pathways, which focused on GPR124 and GPR125.[85–89] In particular for GPR124, it has been shown that this

interplay facilates angiogenesis in the central nervous system.[86,89–91] Since ADGRs and their interacting partners (e.g., synaptic scaffold proteins, see above) are localized at both the pre- and postsynapse, it is conceivable that ADGRs act together with WLS in the transsynaptic translocation of the Wnt1 ligand.[92]

Other Wnt-related interactors identified in TAPs differ between the ADGRs analyzed. However, all Wnt-related interactors indicate a modulating role in Wnt signaling. The most Wnt-related preys were identified in TAPs with VLGR1 constructs. These include molecules previously linked to Wnt signaling, such as ATP6AP2 and PTK7. As a planar cell polarity (PCP) core protein, ATP6AP2 also interacts with another ADGR, namely CELSR1.[93–95] PTK7 is a regulator of both canonical and noncanonical (PCP) Wnt signaling, and like VLGR1 it is essential for hair cell development in the cochlea.[96–98]

For GPR124_CTF and VLGR1_CTF, we also identified SLC30A9, which directly interacts with β-catenin and is part of a complex that activates Wnt-responsive gene transcription.[99,100] Importantly, the transcriptional regulator FHL2, which we found in the VLGR1_ICD dataset, is part of the same complex. Moreover, GPR124_CTF and BAI2_CTF interacted with AMER1, which negatively regulates Wnt signaling by promoting β-catenin degradation.[101,102] Two additional proteins identified in our TAP datasets, namely NONO and SFPQ, further support the relevance of this finding. The transcriptional activator NONO, which colocalizes with AMER1 at nuclear speckles,[99] was found in TAPs of BAI2_CTF. SFPQ, which forms heterodimers with NONO,[103,104] was found in both the GPR124_CTF and BAI2_CTF datasets.

In summary, our data support the prominent role of GPR124 in the regulation of the Wnt signaling pathway.[86,89–91] In addition, our findings indicate that the crosstalk of ADGRs and Wnt signaling is not only restricted to GPR124 or GPR125[85] but may also be mediated by other ADGRs, namely VLGR1 and BAI2.

Concluding remarks

In conclusion, we identified protein networks related to ADGRs by an affinity capture approach. Our data not only support previous findings but also reveal novel molecular relationships, which suggest novel cellular functions for ADGRs. Our data demonstrate that ADGRs of groups I, II, III, VII, and IX are involved in synaptic processes and are modulators of Wnt signaling. In addition, we found evidence for an association of ADGRs with the γ-secretase complex and cleavage of their ICDs, which may act in transcriptional regulation in the nucleus. Whether ADGRs are substrates of the γ-secretase or other proteases remains to be determined. Moreover, our data indicate that ADGRs may have novel roles associated with the intracellular membranes of the ER and mitochondria, and in particular with the joint protein complexes of the MAMs. In any case, we regard the outcome of the present study as springboard for future investigations that should be carried out in order to understand the complex function of ADGRs in health and disease.

Acknowledgments

This work was supported by the German Research Council DFG FOR 2149/WO 548/8 (U.W.), the FAUN-Stiftung, Nuremberg (U.W.), European Community's Seventh Framework Programme FP7/2009 under Grant Agreement Number 241955 (SYSCILIA) (M.U., U.W.), Foundation Fighting Blindness (FFB) PPA-0717-0719-RAD (M.U., U.W.), and the Kerstan Foundation (M.U.). We thank Ulrike Maas for excellent technical assistance and Drs. Gabriela Aust, Ines Liebscher, and Simone Prömel for kindly providing cDNAs of ADGRs. In addition, we thank Dr. Helen May-Simera for helpful discussions and language editing.

Author contributions

B.K. conducted most of the experiments, analyzed data, and prepared most of the figures for publication. J.R. performed sets of tandem affinity purifications. J.K. contributed to experiments analyzing γ-secretase and MAM complexes. K.B., N.H., and M.U. carried out mass spectrometry analysis and analyzed data. B.K. and U.W. designed the studies and wrote the manuscript. All authors read, contributed to, and approved the final manuscript.

Supporting information

Additional supporting information may be found in the online version of this article.

Table S1. Overlap all ADGRs ClueGO results.xls

Table S2. Occurrence of mitochondrial proteins in RAF1 TAPs.xls

Table S3. Overlap LPHN2 CD97 ClueGO results CRAPome cutout.xls

Figure S1. GO term enrichment analysis of ADGR_CTF TAP preys. GO term enrichment analysis in (a) the category *Cellular Component* and (b) the category *Biological Process* for prey proteins that are identical in all ADGR_CTF TAPs.

Figure S2. GO term enrichment analysis of LPHN2, CD97, and VLGR1 interactors. (a) 196 TAP preys are identical for LPHN2, CD97, and VLGR1 CTFs. (b) GO term enrichment analysis in the category *Cellular Component* and (c) the category *Biological Process* for all 196 proteins.

Competing interests

The authors declare no competing interests.

References

1. Hamann, J. & A.G. Petrenko. 2016. Introduction: history of the adhesion GPCR field. *Handb. Exp. Pharmacol.* **234:** 1–11.
2. Hamann, J., G. Aust, D. Arac, *et al.* 2015. International Union of Basic and Clinical Pharmacology. XCIV. Adhesion G protein-coupled receptors. *Pharmacol. Rev.* **67:** 338–367.
3. Arac, D., A.A. Boucard, M.F. Bolliger, *et al.* 2012. A novel evolutionarily conserved domain of cell-adhesion GPCRs mediates autoproteolysis. *EMBO J.* **31:** 1364–1378.
4. Yona, S., H.H. Lin, W.O. Siu, *et al.* 2008. Adhesion-GPCRs: emerging roles for novel receptors. *Trends Biochem. Sci.* **33:** 491–500.
5. Promel, S., M. Frickenhaus, S. Hughes, *et al.* 2012. The GPS motif is a molecular switch for bimodal activities of adhesion class G protein-coupled receptors. *Cell Rep.* **2:** 321–331.
6. Patra, C., M.J. van Amerongen, S. Ghosh, *et al.* 2013. Organ-specific function of adhesion G protein-coupled receptor GPR126 is domain-dependent. *Proc. Natl. Acad. Sci. USA* **110:** 16898–16903.
7. Okajima, D., G. Kudo & H. Yokota. 2010. Brain-specific angiogenesis inhibitor 2 (BAI2) may be activated by proteolytic processing. *J. Recept. Signal Transduct. Res.* **30:** 143–153.
8. Paavola, K.J., J.R. Stephenson, S.L. Ritter, *et al.* 2011. The N terminus of the adhesion G protein-coupled receptor GPR56 controls receptor signaling activity. *J. Biol. Chem.* **286:** 28914–28921.
9. Ward, Y., R. Lake, J.J. Yin, C.D. Heger, *et al.* 2011. LPA receptor heterodimerizes with CD97 to amplify LPA-initiated RHO-dependent signaling and invasion in prostate cancer cells. *Cancer Res.* **71:** 7301–7311.
10. Stephenson, J.R., K.J. Paavola, S.A. Schaefer, *et al.* 2013. Brain-specific angiogenesis inhibitor-1 signaling, regulation, and enrichment in the postsynaptic density. *J. Biol. Chem.* **288:** 22248–22256.
11. Paavola, K.J. & R.A. Hall. 2012. Adhesion G protein-coupled receptors: signaling, pharmacology, and mechanisms of activation. *Mol. Pharmacol.* **82:** 777–783.
12. Langenhan, T., G. Aust & J. Hamann. 2013. Sticky signaling—adhesion class G protein-coupled receptors take the stage. *Sci. Signal.* **6:** re3.
13. Liebscher, I., J. Schon, S.C. Petersen, *et al.* 2014. A tethered agonist within the ectodomain activates the adhesion G protein-coupled receptors GPR126 and GPR133. *Cell Rep.* **9:** 2018–2026.
14. Liebscher, I. & T. Schoneberg. 2016. Tethered agonism: a common activation mechanism of adhesion GPCRs. *Handb. Exp. Pharmacol.* **234:** 111–125.
15. Kishore, A. & R.A. Hall. 2016. Versatile signaling activity of adhesion GPCRs. *Handb. Exp. Pharmacol.* **234:** 127–146.
16. Purcell, R.H. & R.A. Hall. 2018. Adhesion G protein-coupled receptors as drug targets. *Annu. Rev. Pharmacol. Toxicol.* **58:** 429–449.
17. Knapp, B. & U. Wolfrum. 2016. Adhesion GPCR-related protein networks. *Handb. Exp. Pharmacol.* **234:** 147–178.
18. Gloeckner, C.J., K. Boldt & M. Ueffing. 2009. Strep/FLAG tandem affinity purification (SF-TAP) to study protein interactions. *Curr. Protoc. Protein Sci.* Chapter 19: Unit19 20. http://doi.org/10.1002/0471140864.ps1920s57.
19. Boldt, K., J. van Reeuwijk, Q. Lu, *et al.* 2016. An organelle-specific protein landscape identifies novel diseases and molecular mechanisms. *Nat. Commun.* **7:** 11491.
20. Daulat, A.M., P. Maurice, C. Froment, *et al.* 2007. Purification and identification of G protein-coupled receptor protein complexes under native conditions. *Mol. Cell. Proteomics* **6:** 835–844.
21. Atwood, B.K., J. Lopez, J. Wager-Miller, *et al.* 2011. Expression of G protein-coupled receptors and related proteins in HEK293, AtT20, BV2, and N18 cell lines as revealed by microarray analysis. *BMC Genomics* **12:** 14.
22. Gloeckner, C.J., K. Boldt, A. Schumacher, *et al.* 2007. A novel tandem affinity purification strategy for the efficient isolation and characterisation of native protein complexes. *Proteomics* **7:** 4228–4234.
23. Mellacheruvu, D., Z. Wright, A.L. Couzens, *et al.* 2013. The CRAPome: a contaminant repository for affinity purification-mass spectrometry data. *Nat. Methods* **10:** 730–736.
24. Adler, J. & I. Parmryd. 2010. Quantifying colocalization by correlation: the Pearson correlation coefficient is superior to the Mander's overlap coefficient. *Cytometry A* **77:** 733–742.
25. Bhatia, V.N., D.H. Perlman, C.E. Costello & M.E. McComb. 2009. Software tool for researching annotations of proteins: open-source protein annotation software with data visualization. *Anal. Chem.* **81:** 9819–9823.
26. Bindea, G., B. Mlecnik, H. Hackl, *et al.* 2009. ClueGO: a Cytoscape plug-in to decipher functionally grouped gene

ontology and pathway annotation networks. *Bioinformatics* **25:** 1091–1093.
27. Vance, J.E. 2014. MAM (mitochondria-associated membranes) in mammalian cells: lipids and beyond. *Biochim. Biophys. Acta* **1841:** 595–609.
28. Clemente, P., S. Peralta, A. Cruz-Bermudez, *et al*. 2013. hCOA3 stabilizes cytochrome c oxidase 1 (COX1) and promotes cytochrome c oxidase assembly in human mitochondria. *J. Biol. Chem.* **288:** 8321–8331.
29. Molina-Gomes, D., N. Bonnefoy, V.C. Nguyen, *et al.* 1995. The OXA1L gene that controls cytochrome oxidase assembly maps to the 14q11.2 region of the human genome. *Genomics* **30:** 396–398.
30. Mick, D.U., S. Dennerlein, H. Wiese, *et al*. 2012. MITRAC links mitochondrial protein translocation to respiratory-chain assembly and translational regulation. *Cell* **151:** 1528–1541.
31. Saada, A., S. Edvardson, M. Rapoport, *et al*. 2008. C6ORF66 is an assembly factor of mitochondrial complex I. *Am. J. Hum. Genet.* **82:** 32–38.
32. Saada, A., R.O. Vogel, S.J. Hoefs, *et al.* 2009. Mutations in NDUFAF3 (C3ORF60), encoding an NDUFAF4 (C6ORF66)-interacting complex I assembly protein, cause fatal neonatal mitochondrial disease. *Am. J. Hum. Genet.* **84:** 718–727.
33. Heide, H., L. Bleier, M. Steger, *et al*. 2012. Complexome profiling identifies TMEM126B as a component of the mitochondrial complex I assembly complex. *Cell Metab.* **16:** 538–549.
34. Moran, M., L. Marin-Buera, M.C. Gil-Borlado, *et al*. 2010. Cellular pathophysiological consequences of BCS1L mutations in mitochondrial complex III enzyme deficiency. *Hum. Mutat.* **31:** 930–941.
35. van der Laan, M., S.E. Horvath & N. Pfanner. 2016. Mitochondrial contact site and cristae organizing system. *Curr. Opin. Cell Biol.* **41:** 33–42.
36. Stiburek, L., J. Cesnekova, O. Kostkova, *et al*. 2012. YME1L controls the accumulation of respiratory chain subunits and is required for apoptotic resistance, cristae morphogenesis, and cell proliferation. *Mol. Biol. Cell* **23:** 1010–1023.
37. Cipolat, S., T. Rudka, D. Hartmann, *et al*. 2006. Mitochondrial rhomboid PARL regulates cytochrome c release during apoptosis via OPA1-dependent cristae remodeling. *Cell* **126:** 163–175.
38. Pinho, C.M., P.F. Teixeira & E. Glaser. 2014. Mitochondrial import and degradation of amyloid-β peptide. *Biochim. Biophys. Acta* **1837:** 1069–1074.
39. Schreiner, B., L. Hedskog, B. Wiehager & M. Ankarcrona. 2015. Amyloid-β peptides are generated in mitochondria-associated endoplasmic reticulum membranes. *J. Alzheimers Dis.* **43:** 369–374.
40. Leal, N.S., B. Schreiner, C.M. Pinho, *et al*. 2016. Mitofusin-2 knockdown increases ER–mitochondria contact and decreases amyloid β-peptide production. *J. Cell. Mol. Med.* **20:** 1686–1695.
41. Zhou, S., H. Zhou, P.J. Walian & B.K. Jap. 2005. CD147 is a regulatory subunit of the gamma-secretase complex in Alzheimer's disease amyloid beta-peptide production. *Proc. Natl. Acad. Sci. USA* **102:** 7499–7504.
42. Weihofen, A., K. Binns, M.K. Lemberg, *et al*. 2002. Identification of signal peptide peptidase, a presenilin-type aspartic protease. *Science* **296:** 2215–2218.
43. Moliaka, Y.K., A. Grigorenko, D. Madera & E.I. Rogaev. 2004. Impas 1 possesses endoproteolytic activity against multipass membrane protein substrate cleaving the presenilin 1 holoprotein. *FEBS Lett*. **557:** 185–192.
44. Langosch, D., C. Scharnagl, H. Steiner & M.K. Lemberg. 2015. Understanding intramembrane proteolysis: from protein dynamics to reaction kinetics. *Trends Biochem. Sci.* **40:** 318–327.
45. Tomson, B.N. & K.M. Arndt. 2013. The many roles of the conserved eukaryotic Paf1 complex in regulating transcription, histone modifications, and disease states. *Biochim. Biophys. Acta* **1829:** 116–126.
46. Kosugi, S., M. Hasebe, M. Tomita & H. Yanagawa. 2009. Systematic identification of cell cycle-dependent yeast nucleocytoplasmic shuttling proteins by prediction of composite motifs. *Proc. Natl. Acad. Sci. USA* **106:** 10171–10176.
47. Chen, Y.H., C.K. Yang, M. Xia, *et al.* 2007. Role of GAC63 in transcriptional activation mediated by beta-catenin. *Nucleic Acids Res.* **35:** 2084–2092.
48. Reiners, J., E. van Wijk, T. Marker, *et al.* 2005. Scaffold protein harmonin (USH1C) provides molecular links between Usher syndrome type 1 and type 2. *Hum. Mol. Genet.* **14:** 3933–3943.
49. van Wijk, E., B. van der Zwaag, T. Peters, *et al*. 2006. The DFNB31 gene product whirlin connects to the Usher protein network in the cochlea and retina by direct association with USH2A and VLGR1. *Hum. Mol. Genet.* **15:** 751–765.
50. Reiners, J., K. Nagel-Wolfrum, K. Jurgens, *et al*. 2006. Molecular basis of human Usher syndrome: deciphering the meshes of the Usher protein network provides insights into the pathomechanisms of the Usher disease. *Exp. Eye Res.* **83:** 97–119.
51. Yamamoto, Y., K. Irie, M. Asada, *et al*. 2004. Direct binding of the human homologue of the *Drosophila* disc large tumor suppressor gene to seven-pass transmembrane proteins, tumor endothelial marker 5 (TEM5), and a novel TEM5-like protein. *Oncogene* **23:** 3889–3897.
52. Hilbig, D., D. Sittig, F. Hoffmann, *et al.* 2018. Mechanodependent phosphorylation of the PDZ-binding motif of CD97/ADGRE5 modulates cellular detachment. *Cell Rep.* **24:** 1986–1995.
53. Langenhan, T., X. Piao & K.R. Monk. 2016. Adhesion G protein-coupled receptors in nervous system development and disease. *Nat. Rev. Neurosci.* **17:** 550–561.
54. Wu, H., C. Reissner, S. Kuhlendahl, *et al*. 2000. Intramolecular interactions regulate SAP97 binding to GKAP. *EMBO J*. **19:** 5740–5751.
55. Stephenson, J.R., R.H. Purcell & R.A. Hall. 2014. The BAI subfamily of adhesion GPCRs: synaptic regulation and beyond. *Trends Pharmacol. Sci.* **35:** 208–215.
56. Washbourne, P., X.B. Liu, E.G. Jones & A.K. McAllister. 2004. Cycling of NMDA receptors during trafficking in

neurons before synapse formation. *J. Neurosci.* **24:** 8253–8264.
57. Silva, J.P., V.G. Lelianova, Y.S. Ermolyuk, *et al*. 2011. Latrophilin 1 and its endogenous ligand Lasso/teneurin-2 form a high-affinity transsynaptic receptor pair with signaling capabilities. *Proc. Natl. Acad. Sci. USA* **108:** 12113–12118.
58. O'Sullivan, M.L., J. de Wit, J.N. Savas, *et al*. 2012. FLRT proteins are endogenous latrophilin ligands and regulate excitatory synapse development. *Neuron* **73:** 903–910.
59. Specht, D., S.B. Wu, P. Turner, *et al*. 2009. Effects of presynaptic mutations on a postsynaptic Cacna1s calcium channel colocalized with mGluR6 at mouse photoreceptor ribbon synapses. *Invest. Ophthalmol. Vis. Sci.* **50:** 505–515.
60. Sando, R., E. Bushong, Y. Zhu, *et al*. 2017. Assembly of excitatory synapses in the absence of glutamatergic neurotransmission. *Neuron* **94:** 312–321.e313.
61. Duman, J.G., C.P. Tzeng, Y.K. Tu, *et al*. 2013. The adhesion-GPCR BAI1 regulates synaptogenesis by controlling the recruitment of the Par3/Tiam1 polarity complex to synaptic sites. *J. Neurosci.* **33:** 6964–6978.
62. Kreienkamp, H.J., H. Zitzer, E.D. Gundelfinger, *et al*. 2000. The calcium-independent receptor for alpha-latrotoxin from human and rodent brains interacts with members of the ProSAP/SSTRIP/Shank family of multidomain proteins. *J. Biol. Chem.* **275:** 32387–32390.
63. O'Brien, R.J. & P.C. Wong. 2011. Amyloid precursor protein processing and Alzheimer's disease. *Annu. Rev. Neurosci.* **34:** 185–204.
64. Haapasalo, A. & D.M. Kovacs. 2011. The many substrates of presenilin/γ-secretase. *J. Alzheimers Dis.* **25:** 3–28.
65. Merrick, D., H. Chapin, J.E. Baggs, *et al*. 2012. The γ-secretase cleavage product of polycystin-1 regulates TCF and CHOP-mediated transcriptional activation through a p300-dependent mechanism. *Dev. Cell* **22:** 197–210.
66. Qian, F., A. Boletta, A.K. Bhunia, *et al*. 2002. Cleavage of polycystin-1 requires the receptor for egg jelly domain and is disrupted by human autosomal-dominant polycystic kidney disease 1-associated mutations. *Proc. Natl. Acad. Sci. USA* **99:** 16981–16986.
67. Yu, S., K. Hackmann, J. Gao, *et al*. 2007. Essential role of cleavage of polycystin-1 at G protein-coupled receptor proteolytic site for kidney tubular structure. *Proc. Natl. Acad. Sci. USA* **104:** 18688–18693.
68. Chauvet, V., X. Tian, H. Husson, *et al*. 2004. Mechanical stimuli induce cleavage and nuclear translocation of the polycystin-1 C terminus. *J. Clin. Invest.* **114:** 1433–1443.
69. Low, S.H., S. Vasanth, C.H. Larson, *et al*. 2006. Polycystin-1, STAT6, and P100 function in a pathway that transduces ciliary mechanosensation and is activated in polycystic kidney disease. *Dev. Cell* **10:** 57–69.
70. Luo, R., S.J. Jeong, Z. Jin, *et al*. 2011. G protein-coupled receptor 56 and collagen III, a receptor-ligand pair, regulates cortical development and lamination. *Proc. Natl. Acad. Sci. USA* **108:** 12925–12930.
71. Karpus, O.N., H. Veninga, R.M. Hoek, *et al*. 2013. Shear stress-dependent downregulation of the adhesion-G protein-coupled receptor CD97 on circulating leukocytes upon contact with its ligand CD55. *J. Immunol.* **190:** 3740–3748.
72. Scholz, N., J. Gehring, C. Guan, *et al*. 2015. The adhesion GPCR latrophilin/CIRL shapes mechanosensation. *Cell Rep.* **11:** 866–874.
73. Chen, F., H. Hasegawa, G. Schmitt-Ulms, *et al*. 2006. TMP21 is a presenilin complex component that modulates gamma-secretase but not epsilon-secretase activity. *Nature* **440:** 1208–1212.
74. Pal, A., D. Fontanilla, A. Gopalakrishnan, *et al*. 2012. The sigma-1 receptor protects against cellular oxidative stress and activates antioxidant response elements. *Eur. J. Pharmacol.* **682:** 12–20.
75. Krols, M., G. van Isterdael, B. Asselbergh, *et al*. 2016. Mitochondria-associated membranes as hubs for neurodegeneration. *Acta Neuropathol. (Berl.)* **131:** 505–523.
76. Szabadkai, G., K. Bianchi, P. Varnai, *et al*. 2006. Chaperone-mediated coupling of endoplasmic reticulum and mitochondrial $Ca2^{+}$ channels. *J. Cell Biol.* **175:** 901–911.
77. Rostovtseva, T.K., W. Tan & M. Colombini. 2005. On the role of VDAC in apoptosis: fact and fiction. *J. Bioenerg. Biomembr.* **37:** 129–142.
78. Tagaya, M. & K. Arasaki. 2017. Regulation of mitochondrial dynamics and autophagy by the mitochondria-associated membrane. *Adv. Exp. Med. Biol.* **997:** 33–47.
79. Scorrano, L., M. Ashiya, K. Buttle, *et al*. 2002. A distinct pathway remodels mitochondrial cristae and mobilizes cytochrome c during apoptosis. *Dev. Cell* **2:** 55–67.
80. Gilkerson, R.W., J.M. Selker & R.A. Capaldi. 2003. The cristal membrane of mitochondria is the principal site of oxidative phosphorylation. *FEBS Lett.* **546:** 355–358.
81. Cotter, D., P. Guda, E. Fahy & S. Subramaniam. 2004. MitoProteome: mitochondrial protein sequence database and annotation system. *Nucleic Acids Res.* **32:** D463–D467.
82. Calvo, S.E., K.R. Clauser & V.K. Mootha. 2016. MitoCarta2.0: an updated inventory of mammalian mitochondrial proteins. *Nucleic Acids Res.* **44:** D1251–D1257.
83. Pierce, K.L., R.T. Premont & R.J. Lefkowitz. 2002. Seven-transmembrane receptors. *Nat. Rev. Mol. Cell Biol.* **3:** 639–650.
84. Yoon, S. & R. Seger. 2006. The extracellular signal-regulated kinase: multiple substrates regulate diverse cellular functions. *Growth Factors* **24:** 21–44.
85. Li, X., I. Roszko, D.S. Sepich, *et al*. 2013. Gpr125 modulates Dishevelled distribution and planar cell polarity signaling. *Development* **140:** 3028–3039.
86. Zhou, Y. & J. Nathans. 2014. Gpr124 controls CNS angiogenesis and blood–brain barrier integrity by promoting ligand-specific canonical wnt signaling. *Dev. Cell* **31:** 248–256.
87. Li, Q., A. Kannan, A. Das, *et al*. 2013. WNT4 acts downstream of BMP2 and functions via β-catenin signaling pathway to regulate human endometrial stromal cell differentiation. *Endocrinology* **154:** 446–457.
88. Morgan, R., A.M. El-Kadi & C. Theokli. 2003. Flamingo, a cadherin-type receptor involved in the Drosophila planar polarity pathway, can block signaling via the canonical wnt pathway in *Xenopus laevis*. *Int. J. Dev. Biol.* **47:** 245–252.

89. Posokhova, E., A. Shukla, S. Seaman, *et al*. 2015. GPR124 functions as a WNT7-specific coactivator of canonical β-catenin signaling. *Cell Rep.* **10:** 123–130.
90. Vanhollebeke, B., O.A. Stone, N. Bostaille, *et al*. 2015. Tip cell-specific requirement for an atypical Gpr124- and Reck-dependent Wnt/β-catenin pathway during brain angiogenesis. *elife* **4**. http://doi.org/10.7554/eLife.06489.
91. Cho, C., P.M. Smallwood & J. Nathans. 2017. Reck and Gpr124 are essential receptor cofactors for Wnt7a/Wnt7b-specific signaling in mammalian CNS angiogenesis and blood–brain barrier regulation. *Neuron* **95:** 1056–1073.e1055.
92. Korkut, C., B. Ataman, P. Ramachandran, *et al*. 2009. Trans-synaptic transmission of vesicular Wnt signals through Evi/Wntless. *Cell* **139:** 393–404.
93. Buechling, T., K. Bartscherer, B. Ohkawara, *et al*. 2010. Wnt/Frizzled signaling requires dPRR, the *Drosophila* homolog of the prorenin receptor. *Curr. Biol.* **20:** 1263–1268.
94. Hermle, T., M.C. Guida, S. Beck, *et al.* 2013. *Drosophila* ATP6AP2/VhaPRR functions both as a novel planar cell polarity core protein and a regulator of endosomal trafficking. *EMBO J.* **32:** 245–259.
95. Schafer, S.T., J. Han, M. Pena, *et al*. 2015. The Wnt adaptor protein ATP6AP2 regulates multiple stages of adult hippocampal neurogenesis. *J. Neurosci.* **35:** 4983–4998.
96. Lee, J., A. Andreeva, C.W. Sipe, *et al.* 2012. PTK7 regulates myosin II activity to orient planar polarity in the mammalian auditory epithelium. *Curr. Biol.* **22:** 956–966.
97. McGee, J., R.J. Goodyear, D.R. McMillan, *et al*. 2006. The very large G-protein-coupled receptor VLGR1: a component of the ankle link complex required for the normal development of auditory hair bundles. *J. Neurosci.* **26:** 6543–6553.
98. Michalski, N., V. Michel, A. Bahloul, *et al*. 2007. Molecular characterization of the ankle-link complex in cochlear hair cells and its role in the hair bundle functioning. *J. Neurosci.* **27:** 6478–6488.
99. Rivera, M.N., W.J. Kim, J. Wells, *et al*. 2009. The tumor suppressor WTX shuttles to the nucleus and modulates WT1 activity. *Proc. Natl. Acad. Sci. USA* **106:** 8338–8343.
100. Wei, Y., C.A. Renard, C. Labalette, *et al*. 2003. Identification of the LIM protein FHL2 as a coactivator of beta-catenin. *J. Biol. Chem.* **278:** 5188–5194.
101. Grohmann, A., K. Tanneberger, A. Alzner, *et al.* 2007. AMER1 regulates the distribution of the tumor suppressor APC between microtubules and the plasma membrane. *J. Cell Sci.* **120:** 3738–3747.
102. Major, M.B., N.D. Camp, J.D. Berndt, *et al*. 2007. Wilms tumor suppressor WTX negatively regulates WNT/beta-catenin signaling. *Science* **316:** 1043–1046.
103. Shav-Tal, Y. & D. Zipori. 2002. PSF and p54(nrb)/NonO—multi-functional nuclear proteins. *FEBS Lett*. **531:** 109–114.
104. Knott, G.J., C.S. Bond & A.H. Fox. 2016. The DBHS proteins SFPQ, NONO and PSPC1: a multipurpose molecular scaffold. *Nucleic Acids Res.* **44:** 3989–4004.
105. Lewin, T.M., C.G. Van Horn, S.K. Krisans & R.A. Coleman. 2002. Rat liver acyl-CoA synthetase 4 is a peripheral-membrane protein located in two distinct subcellular organelles, peroxisomes, and mitochondrial-associated membrane. *Arch. Biochem. Biophys.* **404:** 263–270.
106. Chiang, S.F., C.Y. Huang, T.Y. Lin, *et al.* 2012. An alternative import pathway of AIF to the mitochondria. *Int. J. Mol. Med.* **29:** 365–372.
107. Goetz, J.G., H. Genty, P. St-Pierre, *et al*. 2007. Reversible interactions between smooth domains of the endoplasmic reticulum and mitochondria are regulated by physiological cytosolic $Ca2^{+}$ levels. *J. Cell Sci.* **120:** 3553–3564.
108. Iwasawa, R., A.L. Mahul-Mellier, C. Datler, *et al.* 2011. Fis1 and Bap31 bridge the mitochondria–ER interface to establish a platform for apoptosis induction. *EMBO J*. **30:** 556–568.
109. Hashimoto, T., R. Hussien & G.A. Brooks. 2006. Colocalization of MCT1, CD147, and LDH in mitochondrial inner membrane of L6 muscle cells: evidence of a mitochondrial lactate oxidation complex. *Am. J. Physiol. Endocrinol. Metab.* **290:** E1237–E1244.
110. Myhill, N., E.M. Lynes, J.A. Nanji, *et al*. 2008. The subcellular distribution of calnexin is mediated by PACS-2. *Mol. Biol. Cell* **19:** 2777–2788.
111. Wang, C.H., Y.F. Chen, C.Y. Wu, *et al*. 2014. Cisd2 modulates the differentiation and functioning of adipocytes by regulating intracellular $Ca2^{+}$ homeostasis. *Hum. Mol. Genet.* **23:** 4770–4785.
112. Browman, D.T., M.E. Resek, L.D. Zajchowski & S.M. Robbins. 2006. Erlin-1 and erlin-2 are novel members of the prohibitin family of proteins that define lipid-raft-like domains of the ER. *J. Cell Sci.* **119:** 3149–3160.
113. Gilady, S.Y., M. Bui, E.M. Lynes, *et al*. 2010. Ero1alpha requires oxidizing and normoxic conditions to localize to the mitochondria-associated membrane (MAM). *Cell Stress Chaperones* **15:** 619–629.
114. Stoica, R., S. Paillusson, P. Gomez-Suaga, *et al*. 2016. ALS/FTD-associated FUS activates GSK-3β to disrupt the VAPB–PTPIP51 interaction and ER–mitochondria associations. *EMBO Rep.* **17:** 1326–1342.
115. Bionda, C., J. Portoukalian, D. Schmitt, *et al.* 2004. Subcellular compartmentalization of ceramide metabolism: mAM (mitochondria-associated membrane) and/or mitochondria? *Biochem. J.* **382:** 527–533.
116. Lynes, E.M., M. Bui, M.C. Yap, *et al.* 2012. Palmitoylated TMX and calnexin target to the mitochondria-associated membrane. *EMBO J.* **31:** 457–470.
117. Hayashi, T. & T.P. Su. 2007. Sigma-1 receptor chaperones at the ER–mitochondrion interface regulate $Ca(2^{+})$ signaling and cell survival. *Cell* **131:** 596–610.
118. Kinoshita, T. & N. Inoue. 2000. Dissecting and manipulating the pathway for glycosylphos-phatidylinositol-anchor biosynthesis. *Curr. Opin. Chem. Biol.* **4:** 632–638.
119. Rusinol, A.E., Z. Cui, M.H. Chen & J.E. Vance. 1994. A unique mitochondria-associated membrane fraction from rat liver has a high capacity for lipid synthesis and contains pre-Golgi secretory proteins including nascent lipoproteins. *J. Biol. Chem.* **269:** 27494–27502.
120. Horner, S.M., H.M. Liu, H.S. Park, *et al.* 2011. Mitochondrial-associated endoplasmic reticulum membranes (MAM) form innate immune synapses and are

targeted by hepatitis C virus. *Proc. Natl. Acad. Sci. USA* **108:** 14590–14595.
121. Hoffstrom, B.G., A. Kaplan, R. Letso, *et al.* 2010. Inhibitors of protein disulfide isomerase suppress apoptosis induced by misfolded proteins. *Nat. Chem. Biol.* **6:** 900–906.
122. Area-Gomez, E., A.J. de Groof, I. Boldogh, *et al.* 2009. Presenilins are enriched in endoplasmic reticulum membranes associated with mitochondria. *Am. J. Pathol.* **175:** 1810–1816.
123. Stone, S.J. & J.E. Vance. 2000. Phosphatidylserine synthase-1 and -2 are localized to mitochondria-associated membranes. *J. Biol. Chem.* **275:** 34534–34540.
124. Saotome, M., D. Safiulina, G. Szabadkai, *et al.* 2008. Bidirectional $Ca2^{+}$-dependent control of mitochondrial dynamics by the Miro GTPase. *Proc. Natl. Acad. Sci. USA* **105:** 20728–20733.
125. Hubner, C.A. & I. Kurth. 2014. Membrane-shaping disorders: a common pathway in axon degeneration. *Brain* **137:** 3109–3121.
126. Sutendra, G., P. Dromparis, P. Wright, *et al.* 2011. The role of Nogo and the mitochondria-endoplasmic reticulum unit in pulmonary hypertension. *Sci. Transl. Med.* **3:** 88ra55.
127. Man, W.C., M. Miyazaki, K. Chu & J. Ntambi. 2006. Colocalization of SCD1 and DGAT2: implying preference for endogenous monounsaturated fatty acids in triglyceride synthesis. *J. Lipid Res.* **47:** 1928–1939.
128. Jia, Z., Z. Pei, D. Maiguel, *et al.* 2007. The fatty acid transport protein (FATP) family: very long chain acyl-CoA synthetases or solute carriers? *J. Mol. Neurosci.* **33:** 25–31.
129. Pereira, L.A., M.P. Klejman & H.T. Timmers. 2003. Roles for BTAF1 and Mot1p in dynamics of TATA-binding protein and regulation of RNA polymerase II transcription. *Gene* **315:** 1–13.
130. Mitra, P., P.S. Vaughan, J.L. Stein, *et al.* 2001. Purification and functional analysis of a novel leucine-zipper/nucleotide-fold protein, BZAP45, stimulating cell cycle regulated histone H4 gene transcription. *Biochemistry* **40:** 10693–10699.
131. Hiraishi, H., J. Oatman, S.L. Haller, *et al.* 2014. Essential role of eIF5-mimic protein in animal development is linked to control of ATF4 expression. *Nucleic Acids Res.* **42:** 10321–10330.
132. Hutlet, B., N. Theys, C. Coste, *et al.* 2016. Systematic expression analysis of Hox genes at adulthood reveals novel patterns in the central nervous system. *Brain Struct. Funct.* **221:** 1223–1243.
133. Laduron, S., R. Deplus, S. Zhou, *et al.* 2004. MAGE-A1 interacts with adaptor SKIP and the deacetylase HDAC1 to repress transcription. *Nucleic Acids Res.* **32:** 4340–4350.
134. Ruvolo, V., E. Wang, S. Boyle & S. Swaminathan. 1998. The Epstein–Barr virus nuclear protein SM is both a post-transcriptional inhibitor and activator of gene expression. *Proc. Natl. Acad. Sci. USA* **95:** 8852–8857.
135. Taylor Clelland, C.L., B. Levy, J.M. McKie, *et al.* 2000. Cloning and characterization of human PREB; a gene that maps to a genomic region associated with trisomy 2p syndrome. *Mamm. Genome* **11:** 675–681.
136. Steen, H. & D. Lindholm. 2008. Nuclear localized protein-1 (Nulp1) increases cell death of human osteosarcoma cells and binds the X-linked inhibitor of apoptosis protein. *Biochem. Biophys. Res. Commun.* **366:** 432–437.
137. Sheng, K., X. Liang, S. Huang & W. Xu. 2014. The role of histone ubiquitination during spermatogenesis. *Biomed. Res. Int.* **2014:** 870695.
138. Cojocaru, M., A. Bouchard, P. Cloutier, *et al.* 2011. Transcription factor IIS cooperates with the E3 ligase UBR5 to ubiquitinate the CDK9 subunit of the positive transcription elongation factor B. *J. Biol. Chem.* **286:** 5012–5022.
139. Muntean, A.G., J. Tan, K. Sitwala, *et al.* 2010. The PAF complex synergizes with MLL fusion proteins at HOX loci to promote leukemogenesis. *Cancer Cell* **17:** 609–621.
140. Garrett, K.P., T. Aso, J.N. Bradsher, *et al.* 1995. Positive regulation of general transcription factor SIII by a tailed ubiquitin homolog. *Proc. Natl. Acad. Sci. USA* **92:** 7172–7176.
141. Yang, Y., H. Hou, E.M. Haller, *et al.* 2005. Suppression of FOXO1 activity by FHL2 through SIRT1-mediated deacetylation. *EMBO J.* **24:** 1021–1032.
142. Rochman, M., Y. Postnikov, S. Correll, *et al.* 2009. The interaction of NSBP1/HMGN5 with nucleosomes in euchromatin counteracts linker histone-mediated chromatin compaction and modulates transcription. *Mol. Cell* **35:** 642–656.
143. Deak, M., A.D. Clifton, L.M. Lucocq & D.R. Alessi. 1998. Mitogen- and stress-activated protein kinase-1 (MSK1) is directly activated by MAPK and SAPK2/p38, and may mediate activation of CREB. *EMBO J.* **17:** 4426–4441.
144. Ouwens, D.M., N.D. de Ruiter, G.C. van der Zon, *et al.* 2002. Growth factors can activate ATF2 via a two-step mechanism: phosphorylation of Thr71 through the Ras-MEK-ERK pathway and of Thr69 through RalGDS-Src-p38. *EMBO J.* **21:** 3782–3793.
145. Fujimaki, K., T. Ogihara, D.L. Morris, *et al.* 2015. SET7/9 enzyme regulates cytokine-induced expression of inducible nitric-oxide synthase through methylation of lysine 4 at histone 3 in the islet β cell. *J. Biol. Chem.* **290:** 16607–16618.
146. Jesko, H. & R.P. Strosznajder. 2016. Sirtuins and their interactions with transcription factors and poly(ADP-ribose) polymerases. *Folia Neuropathol.* **54:** 212–233.
147. Pillutla, R.C., A. Shimamoto, Y. Furuichi & A.J. Shatkin. 1999. Genomic structure and chromosomal localization of TCEAL1, a human gene encoding the nuclear phosphoprotein p21/SIIR. *Genomics* **56:** 217–220.
148. Pfister, A.S., K. Tanneberger, A. Schambony & J. Behrens. 2012. Amer2 protein is a novel negative regulator of Wnt/β-catenin signaling involved in neuroectodermal patterning. *J. Biol. Chem.* **287:** 1734–1741.
149. Cruciat, C.M., B. Ohkawara, S.P. Acebron, *et al.* 2010. Requirement of prorenin receptor and vacuolar H^{+}-ATPase-mediated acidification for Wnt signaling. *Science* **327:** 459–463.
150. Zilberberg, A., A. Yaniv & A. Gazit. 2004. The low density lipoprotein receptor-1, LRP1, interacts with the human frizzled-1 (HFz1) and down-regulates the canonical Wnt signaling pathway. *J. Biol. Chem.* **279:** 17535–17542.
151. Murayama, M., S. Tanaka, J. Palacino, *et al.* 1998. Direct association of presenilin-1 with beta-catenin. *FEBS Lett.* **433:** 73–77.

152. Bin-Nun, N., H. Lichtig, A. Malyarova, *et al.* 2014. PTK7 modulates Wnt signaling activity via LRP6. *Development* **141:** 410–421.
153. Tang, L.Y., N. Deng, L.S. Wang, *et al.* 2007. Quantitative phosphoproteome profiling of Wnt3a-mediated signaling network: indicating the involvement of ribonucleoside-diphosphate reductase M2 subunit phosphorylation at residue serine 20 in canonical Wnt signal transduction. *Mol. Cell. Proteomics* **6:** 1952–1967.
154. Latres, E., D.S. Chiaur & M. Pagano. 1999. The human F box protein beta-Trcp associates with the Cul1/Skp1 complex and regulates the stability of beta-catenin. *Oncogene* **18:** 849–854.
155. Hay-Koren, A., M. Caspi, A. Zilberberg & R. Rosin-Arbesfeld. 2011. The EDD E3 ubiquitin ligase ubiquitinates and up-regulates beta-catenin. *Mol. Biol. Cell* **22:** 399–411.
156. Lui, T.T., C. Lacroix, S.M. Ahmed, *et al.* 2011. The ubiquitin-specific protease USP34 regulates axin stability and Wnt/β-catenin signaling. *Mol. Cell. Biol.* **31:** 2053–2065.
157. Bartscherer, K., N. Pelte, D. Ingelfinger & M. Boutros. 2006. Secretion of Wnt ligands requires Evi, a conserved transmembrane protein. *Cell* **125:** 523–533.